chemosensors

MDPI

Review

Squaraine-Based Optical Sensors: Designer Toolbox for Exploring Ionic and Molecular Recognitions

Daniel D. Ta and Sergei V. Dzyuba *

Department of Chemistry and Biochemistry, Texas Christian University, Fort Worth, TX 76129, USA; DANIEL.TA@tcu.edu
* Correspondence: s.dzyuba@tcu.edu

Abstract: Small molecule-based chromogenic and fluorogenic probes play an indispensable role in many sensing applications. Ideal optical chemosensors should provide selectivity and sensitivity towards a variety of analytes. Synthetic accessibility and attractive photophysical properties have made squaraine dyes an enticing platform for the development of chemosensors. This review highlights the versatility of modular assemblies of squaraine-based chemosensors and chemodosimeters that take advantage of the availability of various structurally and functionally diverse recognition motifs, as well as utilizing additional recognition capabilities due to the unique structural features of the squaraine ring.

Keywords: squaric acid; squarylium; absorbance; fluorescence; aggregation; chelate; chemodosimeter; host–guest chemistry

Citation: Ta, D.D.; Dzyuba, S.V. Squaraine-Based Optical Sensors: Designer Toolbox for Exploring Ionic and Molecular Recognitions. *Chemosensors* **2021**, *9*, 302. https://doi.org/10.3390/chemosensors9110302

Academic Editor: Yinyin Bao

Received: 30 September 2021
Accepted: 21 October 2021
Published: 25 October 2021

1. Introduction: A Case for Squaraine Scaffold

The design and synthesis of small molecule sensors, whose photophysical properties are altered upon interaction with various analytes in differing types of environments, represents one of the most important and active areas of modern chemical research. The tunability of both photophysical properties as well as analyte recognition motifs is crucial for achieving versatile chemosensor designs. Therefore, important consideration lies in the synthetic accessibility of the sensor's scaffold. These facile, modular routes, based on a minimum number of synthetic steps utilizing readily available materials, are among the scaffold's most desirable features.

Squaraine dyes (also known as squarylium dyes or 1,3-squaraines) are resonance-stabilized zwitterionic structures that feature donor–acceptor–donor motifs (Figure 1). Squaraines possess several attractive photophysical characteristics, which include strong absorption in the visible–near-infrared (IR) range, emissions in the near-IR region, good quantum yields, as well as good photostabilities. This contributes to their wide use as photonic materials in a variety of fields, including photovoltaics, biological imaging, and labeling, as well as photodynamic therapy [1,2].

From the synthetic standpoint, it could be argued that squaraine dyes are among the easiest ones to access, since the squaraine scaffold could be assembled in a fairly facile and modular manner. Thus, based on the photophysical properties of squaraines, and their synthetic accessibility, squaraines could be placed among the most versatile dyes that are currently available.

A number of reviews have covered the sensing ability of squaraine dyes in a variety of settings and for numerous analytes [3–7]. Yet, often, the recognition of analytes by the sensors is presented from the analyte perspective, while synthetic aspects for the design of chemosensors are given a lesser priority. Arguably, considering how various structural and functional components could be conjugated to a chromophoric/fluorophoric scaffold might provide a more general approach for more efficient sensor design. The dye's scaffold should provide ample modification points that are amenable to the introduction of multiple

desired functionalities. Despite its fairly simple structure, the squaraine scaffold is fully amenable to diverse functionalization, both pre- and post-squaraine assembly.

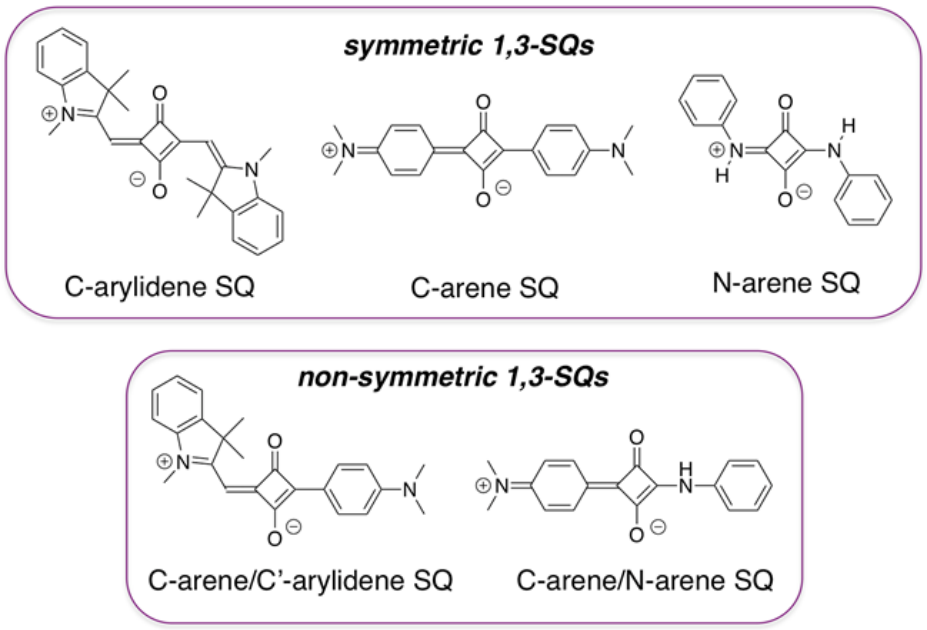

Figure 1. General structures of symmetric and non-symmetric 1,3-squaraines shown in the form of zwitterions. C, C′, and N indicate the nature of the bond that connects squaraine ring to the substituents.

This review will highlight some of the structural and functional motifs that have been used for assembling squaraine-based chemosensors, as an inspiration and a driving force for future designs. It should be mentioned that some of the chemosensors that are presented here could be more accurately described as chemodosimeters [8], based on their covalent interaction with the analyte. However, for the sake of consistency, and uniformity in structure labels, all squaraine-based scaffolds that interact with any analyte, regardless of whether this interaction is covalent or non-covalent in nature, will be referred to as squaraine sensors (**SQS**s).

2. Synthesis of Squaraine Dyes: General Considerations

Synthetic approaches to 1,3-squaraines are quite robust and modular, although they are not always very efficient, as the yields of the final dyes typically range from fair to moderate. However, this "shortcoming" is compensated by the operational simplicity of the isolation and purification of squaraines, i.e., in many instances, filtration, recrystallization and/or washing are sufficient for obtaining pure products. Importantly, as the examples that will follow demonstrate, synthesis of the squaraine core is typically performed under fairly mild conditions. This assures a high degree of functional group tolerance in the synthesis of squaraines. A summary of the general considerations for the synthesis of symmetric and non-symmetric squaraine dyes is presented below. For more detailed, substrate-specific synthetic approaches, some recent reviews could be consulted [9–11].

2.1. Squaric Acid-Based Syntheses

The synthesis of squaraine dyes typically involves a condensation reaction that proceeds via the nucleophilic addition of electron-rich (hetero)aromatics, compounds with an activated methyl group, or amines, to the electrophilic center on the squaric acid (Scheme 1). Several solvent systems, typically at elevated temperatures, have been utilized. However, the most commonly used solvents are as follows: (a) mixtures of aromatic hydrocarbons (typically toluene or benzene) and alcohols (typically n-butanol),

with the azeotropic removal of water (this is, by far, the most prevalent system) [12–14]; (b) alcohols, in the presence of trialkylorthoformates, which are used as dehydrating agents [15–17]; (c) typical molecular organic solvents, such as dimethylformamide [18–20]. Non-conventional types of media, such as deep eutectic solvents, have been recently shown to be suitable for the synthesis of squaraine dyes [21]. Furthermore, solvent-free approaches to some squaraine dyes have been introduced [22]. These novel approaches might prove to be a viable complement to traditional synthetic routes to squaraines.

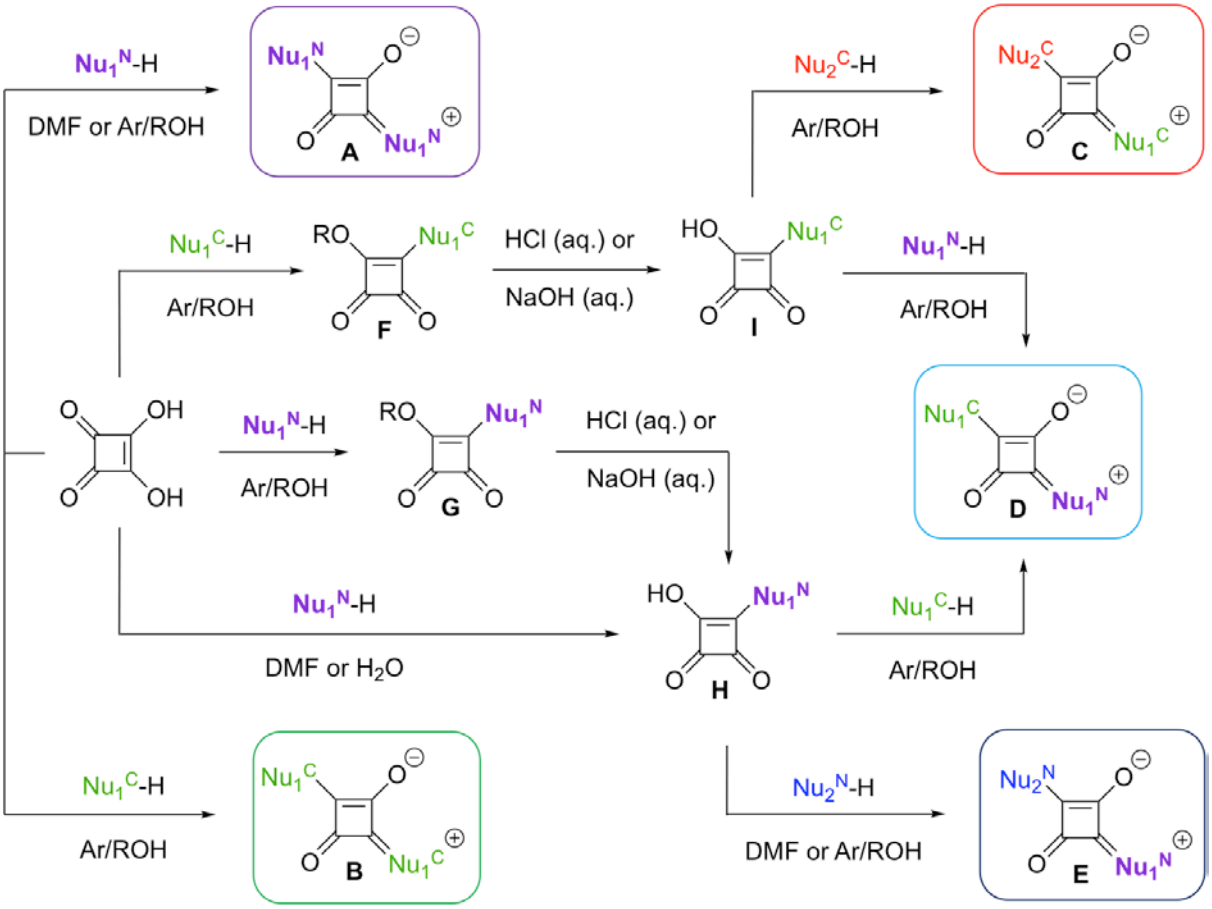

Scheme 1. General synthetic approaches to symmetric and non-symmetric squaraines using squaric acid as the starting material. Nu^C-H and Nu^N-H depict C- and N-nucleophiles, respectively.

Conventionally, the symmetric squaraines **A** and **B** (Scheme 1) are obtained by reacting the corresponding nucleophiles (ca. 2 equiv.) with squaric acid [12–14]. A few general comments are noteworthy. When amines are used as N-nucleophilic components (Nu^N-H), primary amines mostly appear to be viable substrates [12], and only a handful of squaraines are produced upon the reaction of secondary amines with squaric acid [23]. In the case of aromatic amines, the electronic nature of substituents on the aromatic ring appears to have little effect on the efficiency of the reaction. However, only electron-rich aromatic C-nucleophiles (Nu^C-H) prove to be viable reagents for squaric acid; this is consistent with the electrophilic aromatic substitution conditions. For the synthesis of the C-arylidene type of squaraines (Figure 1), condensation reactions typically require the use of organic bases, such as quinolone and pyridine, to generate suitable nucleophilic species.

Understandably, efficient one-pot syntheses of non-symmetric squaraines are not feasible [24]. Therefore, in order to obtain non-symmetrical squaraines, such as **C**, **D**, and **E** (Scheme 1), multistep routes have to be considered. These routes rely on the synthesis of the corresponding semisquaraines, i.e., **H** and **I** [24–26]. Semisquaraine **H** could be obtained directly from the reaction between equimolar amounts of primary amines and

squaric acid. It was found that the reaction is quite facile in water, under both conventional and microwave heating [27,28]. In the case of aromatic amines, the presence of electron-donating and electron-withdrawing groups had little effect on the efficiency of the reaction. In the case of 4-aminobenzylamine [28], the reaction proceeded via the aromatic amine, rather than the benzylic one, due to the protonation of the more basic benzylic amine by squaric acid, thus rendering it non-nucleophilic.

On the other hand, one-step synthesis of the corresponding C-semisquaraine **I** appeared to not be possible, as the reaction between squaric acid and Nu^C-H tends to produce the corresponding alkyl squarate **F** under various conditions [29,30]. However, the subsequent hydrolysis reaction, either under acidic or basic conditions (typically in the presence of organic solvent, such as acetone, EtOH, or AcOH, to aid the solubility of the starting materials) affords **I** in 70–90% yields. It should be noted that the direct conversion of **F** to **C** was also reported [31].

2.2. Squaric Acid Ester and Squaryl Chloride-Based Approaches

In a number of instances, it was reported that general routes that utilize squaric acid as one of the starting materials fail to produce the desired squaraines (e.g., **A** and **B**) and/or semisquaraines **F**, **G**, **H**, and **I** (Scheme 1). Therefore, alternative routes to semisquaraines that involve either dialkyl squarate **J** or squaryl dichloride **K** were developed (Scheme 2).

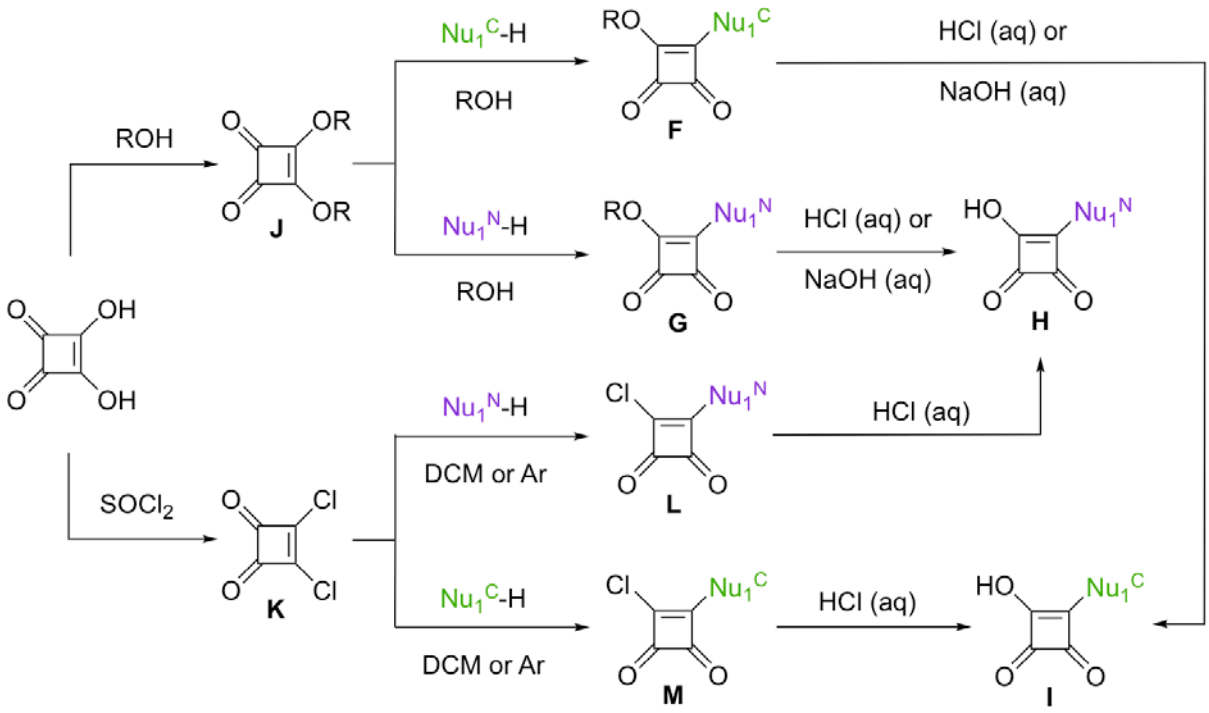

Scheme 2. General synthetic approaches to semisquaraines via dialkyl squarates and squaryl chloride. Nu^C-H and Nu^N-H depict C- and N-nucleophiles, respectively.

Dialkyl squarate **J** is produced via refluxing squaric acid in the corresponding alcohol [32–35], although methyl and ethyl squarates, for example, are available from major chemical manufacturers. The C- and N-containing semisquaric acid esters **F** and **G** could be obtained in ca. 60–80%, upon a reaction of **J** with the corresponding $Nu_1{}^C$-H and $Nu_1{}^N$-H (Scheme 2). These semisquaric acid esters could then undergo hydrolysis, either under acidic or basic conditions, to yield the desired semisquaraines **H** and **I** in moderate to good yields [36–38]. The corresponding squaraines could then be obtained according to general protocols (Scheme 1).

Squaryl chloride **K** could be efficiently produced upon the treatment of squaric acid with chlorinating agents, such as thionyl chloride [39,40], and, typically, as-prepared

K could be used for subsequent steps, without any purification. The reaction between **K** and Nu^{N}_{1}-H or Nu^{C}_{1}-H nucleophiles produces the corresponding semisquaric acid chlorides **L** [41] and **M** [42–45], respectively. The subsequent acidic hydrolysis furnishes semisquaraines **H** and **I** [46–49], which could then be converted to squaraines following established protocols (Scheme 1).

Interestingly, secondary amines, along with primary amines, were shown to be common, viable nucleophiles towards either **J** or **K** [41]. This is contrary to the reaction between amines and squaric acid (Scheme 1), where primary amines were mostly shown to be viable nucleophiles [12].

3. Chelating Group Approach for Sensor Designs

One of the most utilized approaches to chemosensor design relies on the incorporation of an analyte recognition motif into a chromophoric/fluorogenic scaffold (so-called binding unit-signaling unit approach [50]). In the case of squaraine dyes, this approach is realized in a fairly straightforward manner, by utilizing analyte recognition motifs that contain either an electron-rich aromatic moiety or amine functionality. Several analyte-specific recognition motifs, which are primarily based on the so-called host–guest interactions, are given below.

3.1. Crown Ether-Containing Squaraine Sensors

Crown ethers, as well as their nitrogen- and sulfur-containing analogues, are well-known receptors for a variety of alkaline and alkaline-earth (crown and aza-crown ethers), and transition and heavy metals (aza-crown and (aza)-thio-crown ethers) [51]. Synthetic routes to various functional crown ether motifs have been developed, which makes them suitable building blocks for chemosensor development [52]. Crown ether-containing squaraines have been prepared using a general method (Scheme 3) [53], following a condensation reaction between squaric acid and N-phenyl crown ethers [54–56].

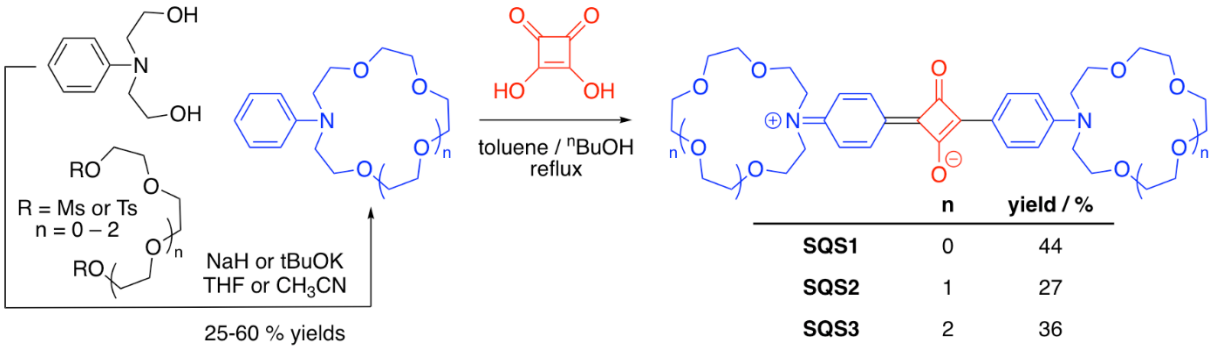

	n	yield / %
SQS1	0	44
SQS2	1	27
SQS3	2	36

Scheme 3. Synthesis of aza-crown ether-containing **SQS1**, **SQS2**, and **SQS3** [53].

The interaction of **SQS1**–**SQS3** was investigated with Li^+, Na^+ and K^+ salts (used as their respective perchlorate salts) in toluene–CH_3CN mixtures. In general, a decrease in both absorption and emission intensities was noted. In addition, by examining the quenching of quantum yield as a function of the increasing concentration of Li^+ and Na^+ salt, it was suggested that **SQS2** forms stronger complexes with these metal ions than **SQS1**. Specifically, **SQS1**–Li and **SQS1**–Na appeared to have K_d values of ca. 3.7 mM and 10 mM [53], respectively, while **SQS2**–Li and **SQS2**–Na appeared to have K_d values of ca. 0.64 and 0.77 mM [57], respectively. Notably, for **SQS1,** a one-to-one complex was prevalent when $[Li^+] \leq 10$ mM, whereas at $[Li^+] > 20$ mM, a two-to-one complex was suggested [57].

Later, the interaction of **SQS1**, **SQS2**, and **SQS3** with alkaline-earth, heavy, and transition metal ions in CH_3CN was investigated using absorption spectroscopy [58]. Only **SQS3** appeared to optically respond to the presence of an equimolar amount of

Ba^{2+}, as was evident by the $\lambda_{ab}{}^{max}$ shift from 636 to 586 nm, with the solution changing color from blue to purple. Qualitatively similar changes in the absorption spectrum of **SQS3** were noted in the presence of Pb^{2+} (although the addition of larger quantities of Pb^{2+} led to the disappearance of the absorption signal). Interestingly, Cu^{2+}, Fe^{3+}, and Hg^{2+} (either in equimolar or excess amounts) induced a color change for all these crown ether-containing sensors. Based on stability constants and semiempirical calculations, it was determined that metal ion coordination at the nitrogen led to hypsochromic shifts, whereas bathochromic shifts were induced by metal ion coordination with the oxygen of the squaraine ring. The coordination of two metal ions typically led to the appearance of a broad band at 480 nm, or bleaching of the signal. However, since complex, yet qualitatively similar profiles were noted in all cases, practical sensing considerations that involve these SQSs might be limited.

One-pot, chromatography-free synthesis of an aza-crown ether-containing squaraine, from commercially available compounds, yielded the dye **SQS4,** with absorption and emission maxima at ca. 635 nm and ca. 665 nm, respectively (Scheme 4) [59]. The 1-Aza-18-crown-6 ionophore on **SQS4** provided some preferential interactions with alkaline-earth metal ions over those of the alkaline ones, with Mg^{2+} and Ba^{2+} ions causing the largest decrease in the absorption and emission intensities of the sensor upon binding. It should be noted that the most pronounced changes were noted when a large excess (ca. 1800-fold) of metal ions, with respect to the sensor **SQS4,** was used. Based on the changes in the absorption spectra of **SQS4**, aggregation of the dye upon binding to Ba^{2+} was evident from the considerable broadening of the signal. Similar spectral changes were noted when the Mg^{2+}–**SQS4** complex was allowed to equilibrate overnight. As a follow-up, a more detailed procedure for **SQS4,** as well as a 1-aza-15-crown-5-containing squaraine, **SQS5**, which should, in principle, have high affinity towards smaller-sized ions, such as Li^{+}, for example, was also reported (albeit no binding studies were disclosed) [60].

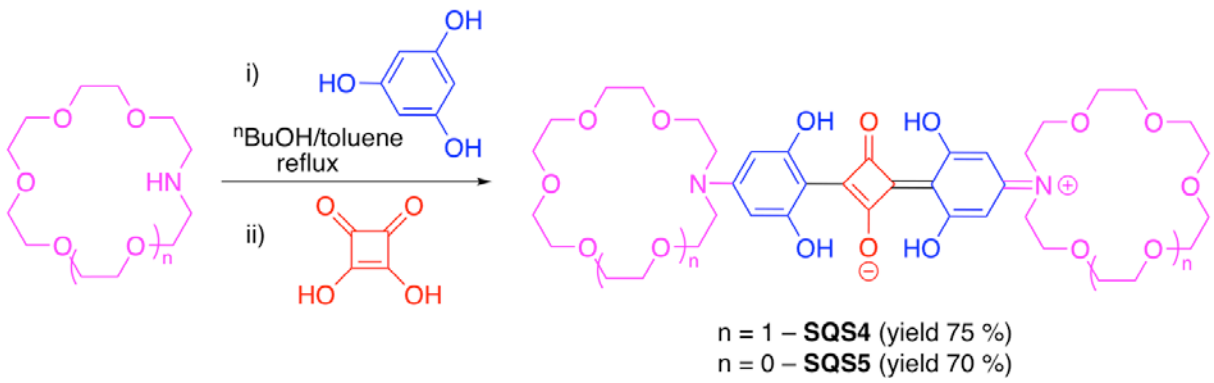

Scheme 4. One-pot synthesis of aza-crown-containing sensors **SQS4** [59] and **SQS5** [60].

Later, it was demonstrated that Li-selective **SQS6** could indeed be obtained by incorporating an aza-15-crown-5 moiety into the squaraine scaffold (Scheme 5) [61]. The synthesis of **SQS6** was accomplished in a fairly straightforward manner, with step 3 proceeding in a 25% yield, while requiring chromatographic purification of **SQS6** (Scheme 5). Specifically, **SQS6** was shown to exhibit a ca. 4.5-fold increase in the emission intensity in the presence of a large excess (up to 500-fold) of Li^{+} ions. It is of interest to point out that even in the presence of a 1000-fold excess of Li^{+}, no significant changes in the absorption spectrum were observed. On the contrary, the absorption spectrum of **SQS6** underwent drastic changes in the presence of even a slight excess of Cu^{2+} ions. Specifically, when **SQS6** (5 μM in CH_2Cl_2/CH_3CN, 1/4 *v/v*, mixture) was titrated with Cu^{2+} (from 5.0 μM to 25 μM; the nature of the Cu salt was not specified), a continuous decrease in absorption intensity, up to ca. 13-fold of the original value, was noted.

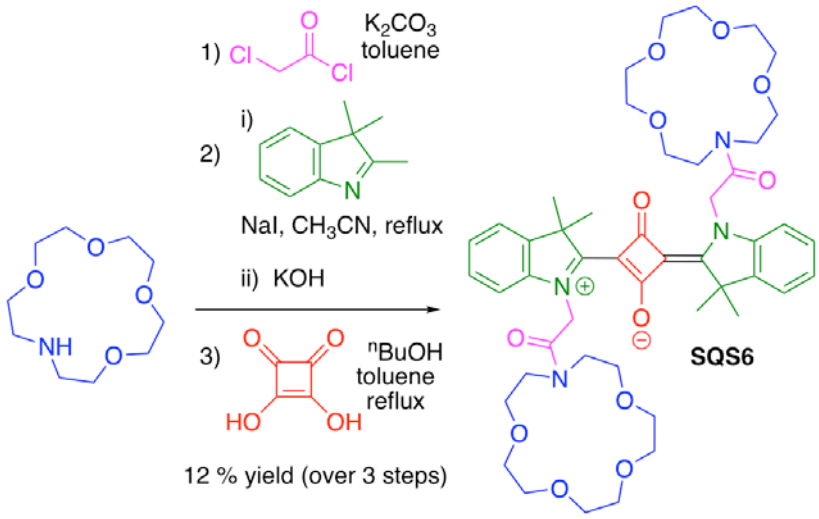

Scheme 5. Synthesis of Li^+-specific **SQS6** [61].

To take advantage of the enhanced binding capabilities of the lariat crown ether, **SQS7** was prepared (Figure 2) [62]. Similarly to the cases described above, a decrease in both the absorption and emission intensities of the sensor took place in the presence of increasing amounts of Na^+ (0 to 4mM), whereas no spectral changes were noted upon the addition of solutions that contained saturated potassium salts, such as nitrate, perchlorate, and thiocyanate. Based on these spectroscopic changes, a dissociation constant of 0.7 mM (in ^{i}PrOH) for the Na–**SQS7** complex was determined.

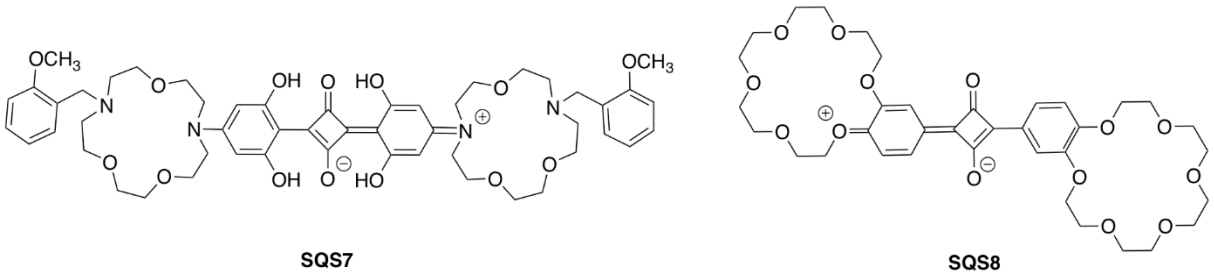

Figure 2. Structures of symmetric lariat diaza-crown ether-containing **SQS7** [62] and benzo-18-crown-6-containing **SQS8** [63].

Although, in general, the complexation of softer Lewis acids, such as Hg^{2+} and Pb^{2+}, would benefit from the presence of softer donor atoms, such as S, dibenzo-18-crown-6-containing **SQS8** (Figure 2) exhibited a relatively high sensitivity towards Hg^{2+}, presumably due to the formation of a sandwich-like complex (based on 1/**SQS8** to 2/Hg^{2+} stoichiometry) [63]. This sensor, which was obtained following a general condensation procedure between an electron-rich aromatic component (i.e., dibenzo-18-crown-6) and squaric acid, showed a typical decrease in absorption intensity in the presence of μM amounts of Hg^{2+} ions. Importantly, no changes in the absorption spectrum of **SQS8** were noted in the presence of other typical host ions for crown ethers, such as Na^+, K^+, and Mg^+, which were all used in a 20-fold molar excess [63].

Sulfur-containing crown ethers are known hosts for a variety of heavy metal ions. Specifically, dithia-dioxa-aza-crown ether (Scheme 6, blue structure), which could be prepared in two steps, using commercially available materials [64], has been widely utilized as a Hg^{2+} and Ag^+ recognition moiety on the fluorescent dye scaffolds, including BODIPY, rhodamine, and anthracene [65]. This crown ether was used to prepare **SQS9**, following a typical condensation procedure (Scheme 6) [66]. In aqueous solution (H_2O:CH_3CN 4:1,

v/v), on the basis of the absorption spectra, both aggregated ($\lambda_{ab}{}^{max}$ = 560 nm; assigned as H-aggregates) and monomeric ($\lambda_{ab}{}^{max}$ = 647 nm) forms of **SQS9** were observed to result in a purple-colored solution. Interestingly, upon the addition of five equivalents of thiophilic cation, such as Hg^{2+}, Pb^{2+}, and Ag^{+}, drastically different spectroscopic responses of **SQS9** were noted. In the presence of Hg^{2+}, complete discoloration of the **SQS9** solution and complete disappearance of the transitions above 500 nm took place. In several CH_3CN/H_2O mixtures, as well as in neat CH_3CN, the limits of Hg^{2+} detection were within the 10–100 nM range. In the presence of Pb^{2+}, no changes were observed. However, Ag^{+} appeared to promote the formation of the monomeric form of **SQS9**, as indicated by the presence of a 647 nm peak, and the formation of a green-colored solution. Not surprisingly, alkali, alkaline-earth, transition, and heavy metal ions (e.g., Li^{+}, Na^{+}, K, Mg^{2+}, Ca^{2+}, Cu^{2+}, Zn^{2+}, Cd^{2+}, Ni^{2+}, Fe^{3+}), i.e., ions with virtually no affinity towards the softer version of crown ethers, did not cause any changes in the absorption spectrum of **SQS9**. The effect of Hg^{2+}/Ag^{+} ions on the emission properties of **SQS9** ($\lambda_{em}{}^{max}$ = 667 nm, Φ = 0.13, τ = 0.67 ns in CH_3CN) was not investigated [66]. It is worth noting that in neat CH_3CN, **SQS9** did show a bathochromic shift in the presence of Fe^{3+} (1 equiv.) and a hypsochromic shift in the presence of Cu^{2+} (1 equiv.) [58].

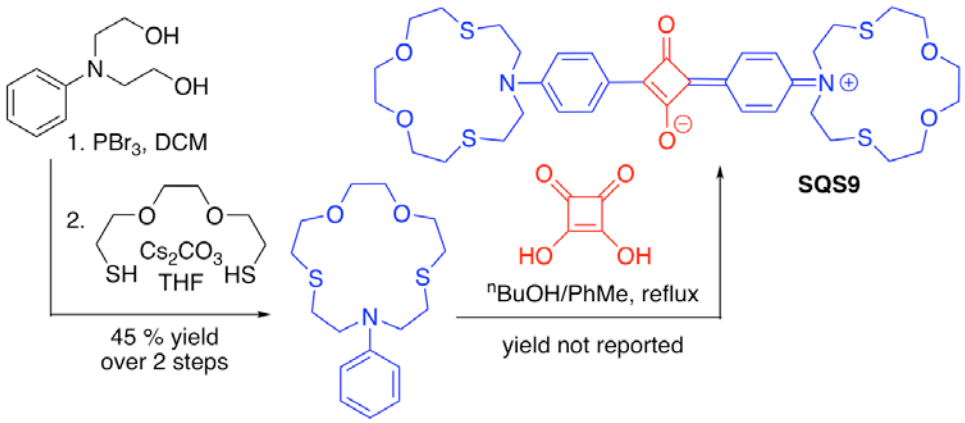

Scheme 6. Synthesis of dithia-crown ether-containing **SQS9** [66] for chromophoric detection of Hg^{2+} and Ag^{+} ions.

Polyether bridged squaraine **SQS10** was synthesized in a straightforward manner, in five steps, starting with catechol (Scheme 7) [67]. Based on dynamic light-scattering data, as well as the absorption and emission profiles of **SQS10** in CH_3CN/H_2O mixtures, **SQS10** was shown to undergo significant aggregation when the water content was $\geq$10% (*v/v*). Thus, all the metal binding studies were conducted in a CH_3CN/H_2O mixture with a 9/1 ratio (*v/v*).

Significant fluorescence enhancement was noted when **SQS10** was titrated with Pb^{2+} salt (K_d = 27 μM), while a number of transition and heavy metal ions, as well as ions that are known typical guests for crown ethers (e.g., Li^{+}, Na^{+}, K^{+}, Mg^{2+}), did not exhibit any prominent increases in emission intensity. It is of interest to mention, however, that the emission intensity of **SQS10** notably increased (ca. four-fold) in the presence of Pb^{2+} (20 equiv.), whereas a ca. seven-fold decrease in emission intensity was noted in the presence of Cu^{2+} (20 equiv.). Thus, **SQS10** could potentially be explored in both "turn-ON" and "turn-OFF" sensing modes [67].

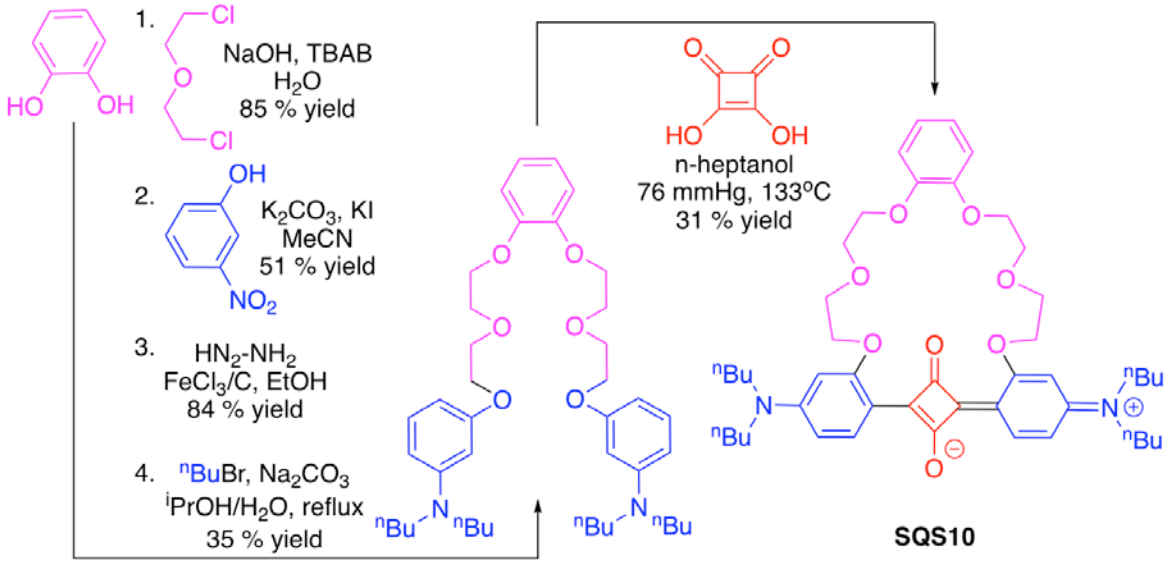

Scheme 7. Synthesis of Pb^{2+}-specific **SQS10** [67].

3.2. Podand-Containing Squaraine Sensors

Podands, acyclic analogues of crown ethers (although other structural scaffolds that are capable of adopting specific geometry around the guest molecule have been included in this group), are among the versatile chelating motifs for various ionic and molecular species [68–70].

The podand-based sensor **SQS11**, with $\lambda_{ab}{}^{max}$ = 630 nm and $\lambda_{em}{}^{max}$ = 652 nm, was obtained in a fairly straightforward manner, via condensation between bis-N-phenyl-containing podand and an aniline-containing semisquaraine (Scheme 8) [71]. In the presence of increasing amounts of Ca^{2+}, the sensor **SQS11** exhibited the following ratiometric response: a decrease in the 630 nm absorption maximum was accompanied by an increase in the 570 nm transition. Furthermore, a pronounced decrease in emission intensity was even noted in sub-equimolar amounts of Ca^{2+}, with a relatively low estimated dissociation constant (K_d 0.53 μM). The observed spectroscopic changes have been attributed to the formation of a foldameric structure, where the two chromophoric squaraine units were brought into close proximity of each other due to Ca-podand complexation, i.e., in the form of a face-to-face π-stacking arrangement. This structure was responsible for the hypsochromic shift, which was consistent with the formation of H-type species.

The sensor **SQS11** showed significant selectivity towards Ca^{2+} in CH_3CN; for example, only insignificant changes in the absorbance and emission spectra of **SQS11** were noted in the presence of Na^+, K^+, Sr^{2+}, Mg^{2+}, or Ba^{2+}. When 0.5 and 1.0 equiv. of Ca^{2+} were added to **SQS11**, the quantum yield decreased by ca. 40 and 97%, respectively. On the contrary, when the same amounts of Mg^{2+} (i.e., 0.5 and 1.0 equiv.) were added, the quantum yield of **SQS11 only** decreased by ca. 5 and 20%, respectively.

By adjusting the length of the ethylene glycol tether, several other podand-containing squaraine sensors, **SQS12–SQS14,** were prepared (Scheme 8) [72]. The spectroscopic characteristics of **SQS12–SQS14** exhibited some dependence on the length of the tether; for example, the absorption and emission maxima showed negative correlations with increasing numbers of ethylene glycol units in the podand moiety, whereas the quantum yields showed a positive correlation.

Notably, different stoichiometries were realized in regard to the Ca–**SQS12** and Mg–**SQS12** complexes. The larger cation Ca^{2+} was not a good fit for the podand's oxygen and two nitrogen coordination sites, which prompted the formation of a sandwich-like two-to-one complex. On the other hand, the smaller cation Mg^{2+} appeared to favor the formation of a one-to-one complex. It should also be noted that as the length of the tether increased,

i.e., **SQS12** to **SQS14**, the formation of one-to-one complexes appeared to be preferred, regardless of the identity of the metal ion. Furthermore, the mono-squaraine-containing podands **PO1**–**PO5** (Scheme 8, bottom left) showed no changes in the absorption and emission spectra in the presence of various alkaline or alkaline-earth metal ions. However, ^{1}H NMR investigations revealed that these podands do interact with Ca^{2+} and Mg^{2+}, while no podand–metal interactions were detected for Li^+, Na^+, or K^+ [72,73].

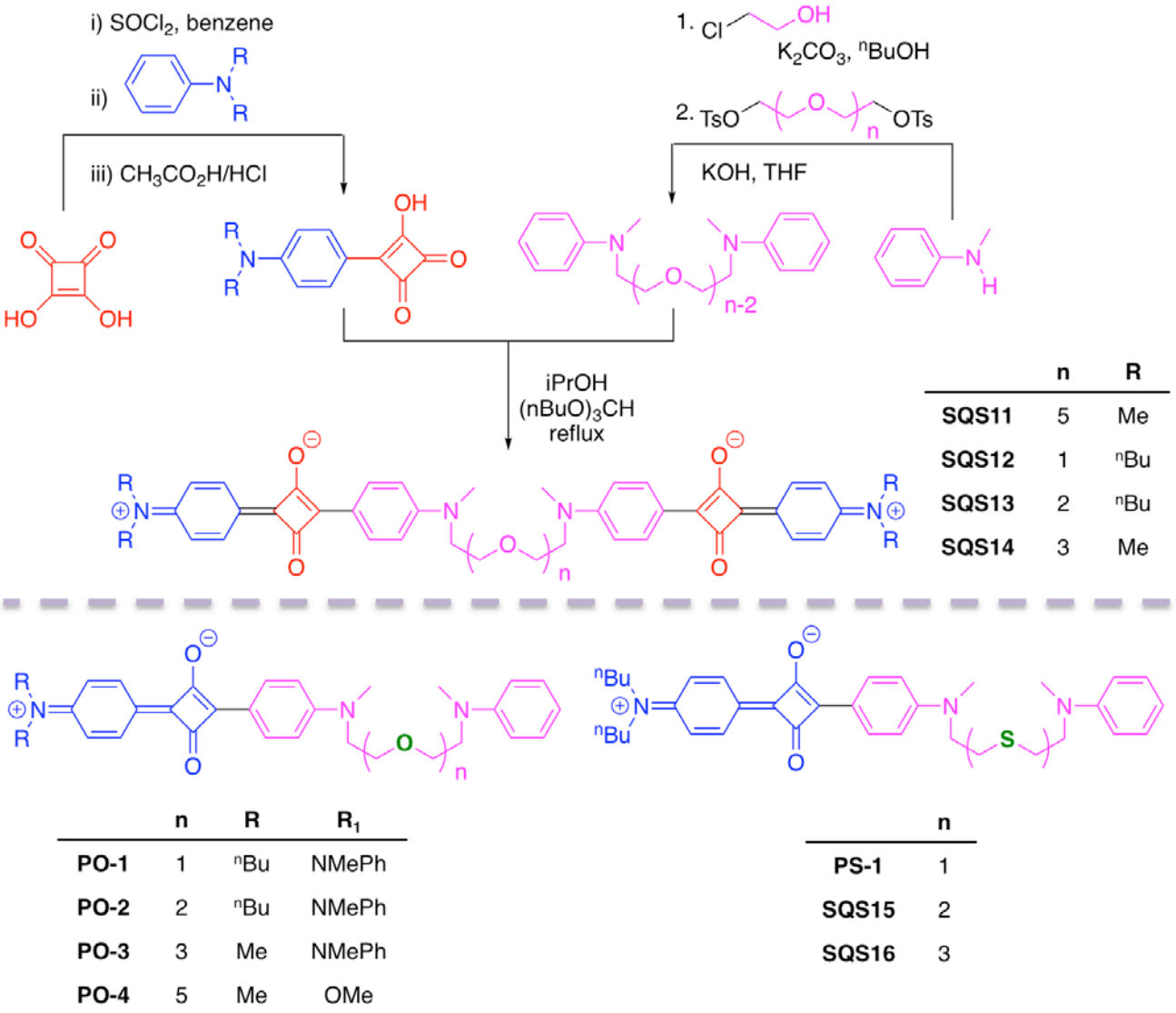

	n	R
SQS11	5	Me
SQS12	1	^{n}Bu
SQS13	2	^{n}Bu
SQS14	3	Me

	n	R	R_1
PO-1	1	^{n}Bu	NMePh
PO-2	2	^{n}Bu	NMePh
PO-3	3	Me	NMePh
PO-4	5	Me	OMe

	n
PS-1	1
SQS15	2
SQS16	3

Scheme 8. Synthesis of podand-containing optical sensors **SQS11**–**SQS14** (top, [71,72]), and examples of optically silent Ca^{2+}/Mg^{2+}–hosts **PO1**–**PO4** (bottom left, [72,73]) and thio-containing **SQS15** and **SQS16**, and thio-containing podand **PS-1** (bottom right, [74]).

The incorporation of soft S-donor atoms into the podand structure is known to favor the coordination of various metal ions that are considered to be soft Lewis acids, including mercury (Hg^{2+}) and silver (Ag^+). Thus, **SQS15** and **SQS16**, along with **PS-1** (Scheme 8, bottom right), were synthesized, and their ability to interact with Hg^{2+} was examined [74]. Unlike the oxygen-containing squaraines **PO1**–**PO4**, which showed no optical response in the presence Ca^{2+}, the thio-containing analogues did show an optical response in the presence of Hg^{2+}, and the sensing ability appeared to be dependent on the length of the podand moiety, with **SQS16** exhibiting the most pronounced changes in the presence of Hg^{2+} (4 equiv.), while **PS-1** was optically silent. Thus, by simply switching the recognition motif,

while retaining the other structural features of the squaraine dye constant, it appeared to be possible to construct sensors that are selective towards distinct analytes.

Additionally, a number of other thio-containing podands, in particular, those containing a thiocarbamate moiety, had been conjugated onto the squaraine's scaffold and produced Hg^{2+}-specific sensors, which appeared to have "turn-ON" responses (Figure 3). Symmetric **SQS17** showed strong absorption ($\lambda_{ab}{}^{max}$ = 644 nm) and emission ($\lambda_{em}{}^{max}$ = 661 nm) bands in organic solvents (CH_2Cl_2, $CHCl_3$, AcOH), which were indicative of a monomeric structure [75]. In aqueous solutions, aggregates of **SQS17** were noted; for example, the purple-colored solution of **SQS17** in the AcOH–H_2O mixture (4/6 *v/v*), with a broad absorption range of 500–700 nm ($\lambda_{ab}{}^{max}$ = 548 nm), showed no transitions above 650 nm in the emission spectrum. However, upon the addition of a Hg^{2+} salt, a change from a purple- to blue-colored solution was noted, with the appearance of an absorption band at 636 nm, and a strong emission at 660 nm. These spectral changes indicated that the complexation of Hg^{2+} induced the formation of the monomeric form of **SQS17**. Importantly, other metals ions, which are also considered to be soft Lewis acids (e.g., Ag^{+}, Cd^{2+}, Pb^{2+}), did not produce any noticeable changes, either in the absorption or in the emission spectra of **SQS17**. This suggested a lack of interaction with **SQS17**, as well as an inability of these ions to induce the disaggregation of **SQS17**. Therefore, **SQS17** appeared to be a viable, selective, naked-eye Hg^{2+} sensor, which provided an emission enhancement of ca. 700-fold, affording a detection limit of 7.1 nM.

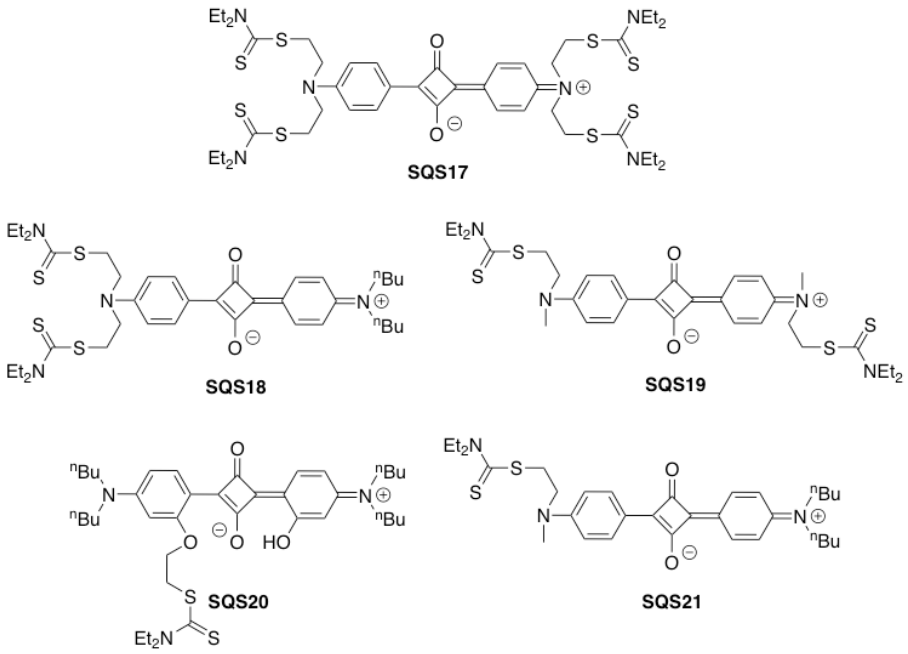

Figure 3. Structures of thiocarbamate-containing **SQS17** [75], **SQS18** [76], **SQS19** [77], **SQS20** [78], **SQS21** [79].

The related non-symmetric **SQS18** maintained high selectivity towards Hg^{2+}, but showed only a 10-fold enhancement in emission intensity in the presence of Hg^{2+} (45 nM detection limit) [76]. For some squaraines, i.e., **SQS19** and **SQS20**, the disaggregation effects induced by Hg^{2+} were amplified by the addition of excess amounts of EDTA [77,78]. It is also of interest to note that even one dithiocarbamate moiety on the squaraine scaffold, i.e., **SQS20** and **SQS21** (Figure 3), still yielded a Hg^{2+}-selective response, with detection limits that were somewhat comparable to **SQS17** [78,79], albeit with significantly reduced emission enhancement observed upon the addition of Hg^{2+} salt; for example, a ca. four-fold increase in emission intensity in the presence of Hg^{2+} (3 equiv.) was observed in the case of **SQS18**, while a ca. 700-fold increase was noted for **SQS17** in the presence of Hg^{2+} (5 equiv.). However, direct comparisons between **SQS17** and **SQS18**

should be taken with caution, due to the differences in the nature and composition of the media that were used for spectroscopic and metal ion detection studies, i.e., AcOH–H_2O (4/6 *v/v*) in the case of **SQS17**, versus EtOH–H_2O (1/4 *v/v*) in the case of **SQS18**. Additional structural manipulation revealed that the position of the dithiocarbamate moiety in the squaraine scaffold, e.g., **SQS20** vs. **SQS21**, had little effect on the sensing ability towards Hg^{2+}; both sensors showed good Hg^{2+} selectivity over other metal ions, and the emission intensity enhancements were in the range of 8- to 10-fold.

In contrast, **SQS22**, **SQS23**, and **SQS24**, which feature thio-ether-containing binding motifs, provided "turn-OFF" responses upon interaction with metal ions (Figure 4) [80–82]. Specifically, in CH_3CN, **SQS22** exhibited the following spectral characteristics that were consistent with monomeric species: a strong, narrow absorption band ($\lambda_{ab}{}^{max}$ = 636 nm) and intense emission ($\lambda_{em}{}^{max}$ = 670 nm) [80]. However, upon addition of $Hg(ClO_4)_2$, a gradual decrease in absorption intensity and a hypsochromic shift of $\lambda_{ab}{}^{max}$ to 575 nm, along with a decrease in emission intensity, were noted (in the presence of 20 equiv. of Hg^{2+}, **SQS22** showed no significant absorption or emission transitions). It is of interest to point out that in the presence of 20 equiv. of Cu^{2+} and Fe^{3+} (but not in the presence of Ag^+, Pb^{2+}, Cd^{2+}, Zn^{2+}, Ni^{2+}, Fe^{2+}, Cr^{3+}), significant changes in both the absorption and emission spectra of **SQS22** were noted. The optical response of **SQS22** to Cu^{2+} was identical to that of Hg^{2+}, whereas, in the presence of Fe^{3+}, a ca. 20 nm hypsochromic shift, with decrease (ca. 1.6-fold) in intensity and moderate broadening, along with a ca. 10-fold decrease in emission intensity, was observed. Yet, in the CH_3CN/H_2O (2/1 *v/v*) mixture, only Hg^{2+} retained its interaction with **SQS22**, while all the other ions, including Cu^{2+} and Fe^{3+}, did not induce any spectral changes in **SQS22**'s optical profiles. Thus, an efficient "turn-OFF" Hg sensor was realized [80]. Under these conditions (i.e., 20 equiv. of Hg^{2+}, 2/1 (*v/v*) CH_3CN/H_2O mixture), the sensing ability of **SQS22**–Hg towards thiophilic species was tested. In the presence of Cys, Hcy, GSH, and His (20 equiv.), significant intensity increases in the absorption (at 642 nm) and emission (at 678 nm) bands were observed, which indicated a "turn-ON" sensing profile.

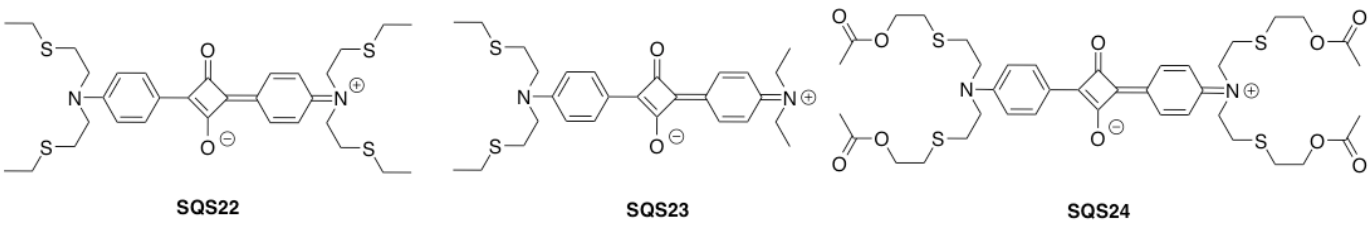

Figure 4. Structures of thio-containing sensors **SQS22** [80], **SQS23** [81], and **SQS24** [82].

The observed cross-sensitivity of **SQS22**–Hg towards both SH-containing analytes and His prompted further studies that led to **SQS23** [81], which was synthesized following the general routes utilized for non-symmetric squaraines (Scheme 2). Similarly to **SQS22**, in aqueous media, **SQS23** was present in the form of non-emissive aggregates, which exhibited a broad absorption band in the 480–780 nm range. Monomer-to-aggregate equilibrium appeared to be dependent on the amount of water in the H_2O/THF mixtures. Importantly, **SQS23**–Hg's Cys-His selectivity could be easily modulated by simply adjusting the water content, with the highest Cys-His selectivity (ca. 6.3-fold) achieved in the 4/1 H_2O/THF mixture. In addition, **SQS23** was found to be completely soluble in the aqueous solution that contained β-cyclodextrin (β-CD), and the formation of the inclusion complex was confirmed by the appearance of an induced circular dichroism signal at 650 nm [81]. Encapsulated **SQS23** showed the following photophysical characteristics that were consistent with the monomeric form of the dye: a narrow absorption band at 648 nm, and a strong emission (quantum yield of 0.28) band at 675 nm. Similarly to the **SQS23**–Hg^{2+} interaction, the **SQS23**–β-CD complex was also able to complex with Hg^{2+}, which was evident from the decreasing absorption and emission bands of **SQS23**–β-CD in

the presence of increasing amounts of Hg^{2+}. In addition, the **SQS23**–β-CD–Hg assembly showed ca. three-fold selectivity towards SH-containing analytes (e.g., Cys, Hcys, and GSH) over His [81].

The incorporation of a slightly more elaborate thio-ether-containing binding motif on the squaraine scaffold yielded **SQS24** (Figure 4) [82]. The monomeric form of **SQS24** was observed in EtOH, yet the formation of J-aggregates (broad peaks with a maximum around 750 nm) was noted in the EtOH/H_2O mixtures with a water content above 70% (*v*/*v*). This sensor showed moderate selectivity towards Ag^+ (ca. 1.4-fold selectivity over other ions) and Hg^{2+} (ca. 3.2-fold selectivity over other ions), as assessed by the changes in emission intensity. It appeared that the "turn-ON" response was induced when EDTA was added to a weakly fluorescent **SQS24**–Hg complex, but not to a **SQS24**–Ag complex. Furthermore, various amino acids, including Cys, His, and Trp, induced a significant increase in both the absorption and emission bands when added to **SQS24**–Hg. This highlighted the inferior selectivity capabilities of **SQS24**–Hg compared to other thio-containing squaraine sensors.

Thus, depending on the structural features within the podand-like moieties, SQSs that operate in either "turn-ON" or "turn-OFF" modes (Figures 3 and 4) towards ionic and molecular analytes could be realized.

3.3. Tetracarboxylate Binding Motif

The introduction of a tetracarboxylate binding motif on two tethered aromatic units produced sensors that allowed for the measurement of cytosolic Ca^{2+}, with high selectivity over other divalent ions, especially Mg^{2+} (Figure 5A) [83,84]. Built on the successful application of these sensors for Ca^{2+} sensing, various fluorophores have been decorated with a tetracarboxylate chelating motif that yielded Ca^{2+} sensors [85]. These sensors offer a wide spectroscopic range, which covers green, red and near-IR regions, in both absorbance and emission, while affording emission enhancements of over 100-fold upon Ca binding [85].

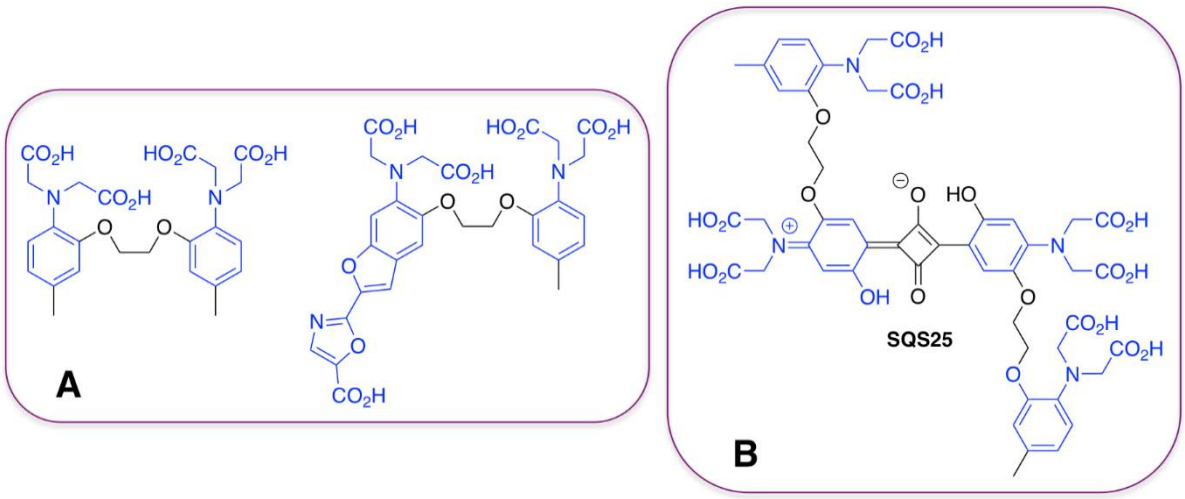

Figure 5. Structures of Ca-specific sensors. (**A**): original Ca indicators; (**B**): squaraine-containing **SQS25** [86].

The incorporation of the tetracarboxylate motif into the squaraine scaffold produced the sensor **SQS25** that exhibited absorption and emission maxima at 698 nm and 733 nm, respectively (Figure 5B) [86]. The construction of **SQS25** was accomplished via a chromatography-free two-step procedure, using typical condensation conditions between squaric acid and the more electron-rich aromatic moiety of the t-Bu-protected tetracarboxyl-containing unit, followed by TFA-induced removal of the t-Bu group (Figure 5B; the tetracarboxyl-aromatic moiety was synthesized via a multi-step chromatography-free sequence).

The intensity of the absorption of **SQS25** underwent continuous decreases upon the addition of increasing amounts of Ca^{2+} ions, with notable changes (ca. 30% decrease) starting to occur in sub-equivalent amounts of Ca^{2+} [86]. At a 500-fold excess of Ca^{2+}, appreciable broadening of the absorption peak at 698 nm (along with a ca. 80% decrease in intensity, and the appearance of additional peaks below 650 nm), indicative of the formation of various aggregation species, was noted. The dissociation constant was determined to be 3.6 μM. Importantly, however, no significant changes in the absorption spectrum of **SQS25** were noted, even in the presence of a large excess (ca. 400-fold) of Mg^{2+}. Notable changes in the presence of Ca^{2+} ions were also present in the emission spectrum of **SQS25** (Figure 5B). About a 30% decrease in emission intensity was observed when a 3.8-fold excess of Ca^{2+} was added, and a large excess of Ca ions led to a further decrease in **SQS25**'s emission signal, with some flattening of the response above a 75-fold excess of Ca^{2+} [86].

3.4. Nitrogen-Containing Heterocycles as Binding Motifs

N-containing heterocycles, in particular, pyridine, are among the most commonly used moieties that are present in a variety of binding motifs for transition and heavy metal ions [87–90]. The incorporation of such pyridine-containing chelators, such as di-2-pyridylmethylamine (i.e., dipicolylamine), in various dye scaffolds is a proven strategy to obtain viable chemosensors [91–93].

The introduction of dipicolyl moieties into the squaraine scaffold, to give **SQS26,** was achieved using a solvent-free, one-step process from commercially available starting materials (Scheme 9) [94]. Notably, although reactions between aliphatic amines and alkyl squarates tend to give squaramides [95], in this particular case, neat conditions at the elevated temperature appeared to favor an exclusive formation of the symmetric 1,3-disubstituted squaraine. In addition, unlike most squaraine dyes, **SQS26** appeared to be completely soluble in water (over a wide pH range), and no aggregation processes were noted, based on ^1H NMR spectroscopy in D_2O over a period of 8 days. Detailed pH and metal ion binding studies using **SQS26** were carried. In addition, a notable (ca. six-fold) increase in the emission intensity of **SQS26** ($\lambda_{em}{}^{max}$ = 476 nm) was observed in the presence of Hg^{2+} (1.05 equiv. added as $Hg(NO_3)_2$ salt in MES buffer (2.5 mM, pH 5.0)). On the other hand, no prominent changes in the emission spectra of **SQS26** were noted in the presence of other metal ions, such as Zn^{2+} and Cu^{2+}, even though these ions are known to complex with the dipicolyl motif.

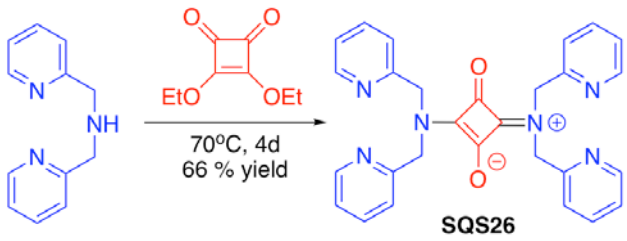

Scheme 9. Solvent-free synthesis of **SQS26** [94].

Other pyridine-containing squaraine-based sensors have also been reported. Specifically, **SQS27** and **SQS28** were prepared in a straightforward manner (Scheme 10) [96]. **SQS27** provided a naked-eye determination of Cu^{2+} ions; the absorption maximum of **SQS27** ($\lambda_{ab}{}^{max}$ = 514 nm; pink-colored solution) underwent a drastic shift to the red region ($\lambda_{ab}{}^{max}$ = 680 nm; blue-colored solution). Upon addition of EDTA, the pink color of **SQS27** was restored, thus indicating a reversible nature of the **SQS27**–Cu interaction. Significantly, no pronounced changes were observed in the presence of 26 metal ions, including alkaline, alkaline-earth, transition, heavy metal, and lanthanides. It was determined that the one-to-one **SQS27**–Cu complex had K_d = 0.5 μM. Furthermore, Cu selectivity was observed when the emission spectra of **SQS27** were recorded in the presence of various metal ions; a six-fold decrease in the emission intensity ($\lambda_{em}{}^{max}$ = 626 nm) was produced in the

presence of only Cu^{2+}. The possibility of **SQS27** having Cu-sensing ability in a biological setting was tested using LL/2 and HepG2 cell lines. A notable decrease in intracellular fluorescence, i.e., "turn-OFF" response, was detected when these cells (incubated with 20 μM **SQS27**) were treated with $CuCl_2$ (100 μM). Virtually complete fluorescence recovery was observed upon addition of EDTA (500 μM).

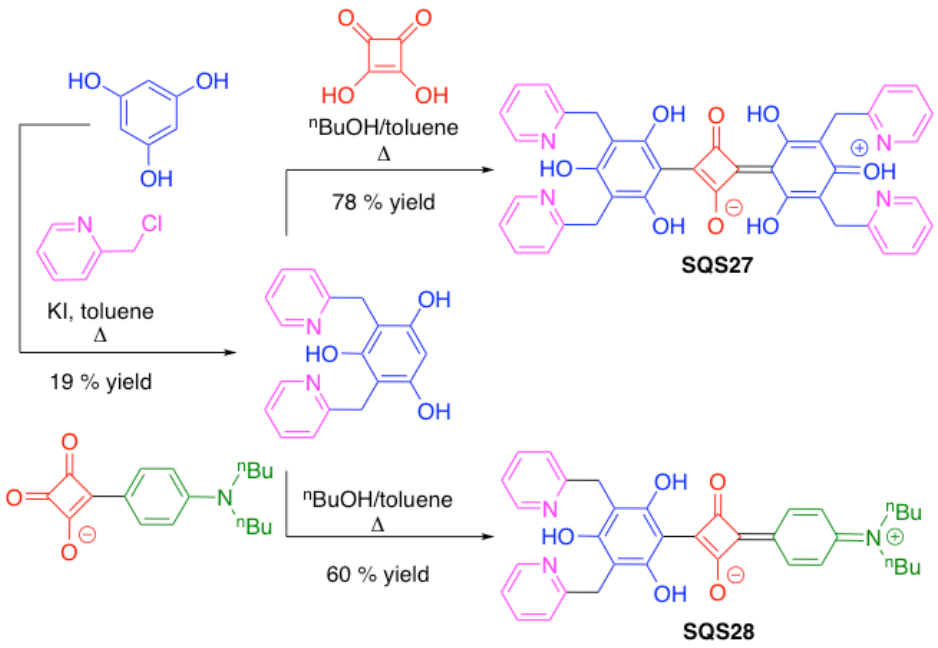

Scheme 10. Synthesis of symmetric **SQS27** and non-symmetric **SQS28** sensors [96].

Similarly, in the presence of Cu^{2+} ions, **SQS28** also exhibited red-shifted absorption, albeit less pronounced (from 554 nm to 640 nm, i.e., 86 nm shift) compared to **SQS27** (166 nm shift), along with a ca. eight-fold suppression in emission intensity at 651 nm.

The incorporation of a quinoline moiety on squaraine's scaffold was achieved in three steps, to give **SQS29** (Scheme 11) [97]. Unlike many squaraines, **SQS29** appeared to be relatively soluble in water, without significant aggregate formation. Specifically, the intensity of a narrow absorption peak ($\lambda_{ab}{}^{max}$ = 645 nm) in ethanol (EtOH, 100%) decreased only by ca. 7% when the water content was increased from 0 to 70%, without any appreciable broadening of the peak or shift of the $\lambda_{ab}{}^{max}$. Although, in 100% water, a ca. 1.8-fold decrease in absorption intensity was observed, neither the width nor the $\lambda_{ab}{}^{max}$ of the peak changed. The fluorescent intensity of **SQS29** ($\lambda_{em}{}^{max}$ = 664 nm) was largely unaffected when the water content varied from 0 to 70% in EtOH.

By screening the interaction of **SQS29** with various metal ions, a "turn-OFF" mode towards Hg^{2+} was observed. The emission intensity gradually decreased in the presence of increasing concentrations of Hg^{2+}; a 10 % decrease was noted in the presence of 4 equiv. of Hg^{2+}, whereas a 90 % decrease was noted in the presence of 24 equiv. of Hg^{2+}. The emission intensity of **SQS29** was restored upon addition of EDTA to **SQS29**–Hg solution (qualitatively similar results were obtained by the addition of a Cys, while GSH and His showed an inferior recovery of **SQS29** emission, i.e., ca. 30% of that achieved with Cys).

Bipyridyl is a common binding motif for a variety of transition and heavy metal ions [90]. The incorporation of bipyridyl into the squaraine scaffold was achieved following a multi-step synthetic route, to give **SQS30** (Scheme 12) [98]. This sensor was prone to aggregation in the presence of water, as the formation of non-emissive, H-type aggregates, with a low molar extinction coefficient, was observed. Thus, all fluorescent studies involving analytes were conducted in acetone. It was found that in the presence of increasing amounts of Zn^{2+} ions, a decrease in the emission maximum at 698 nm, with a

concurrent increase in the maximum at 720 nm, was noted. Furthermore, the absorption spectrum of **SQS30** revealed a bathochromic shift (from 680 nm to 695 nm) in the presence of Zn^{2+}. Based on these spectroscopic data, the detection limit for Zn^{2+} was estimated to be ca. 60 nM. Noteworthy, **SQS30** showed a complex fluorescence emission response to other metal ions; for example, **SQS30** became completely non-emissive above 680 nm in the presence of Cd^{2+}, Cu^{2+}, Co^{2+}, and Ni^{2+}, whereas a ca. 10-fold decrease in emission intensity ($\lambda_{em}{}^{max}$ = 698 nm, i.e., no shift in the **SQS30** maximum) was observed in the presence of Ag^{+}.

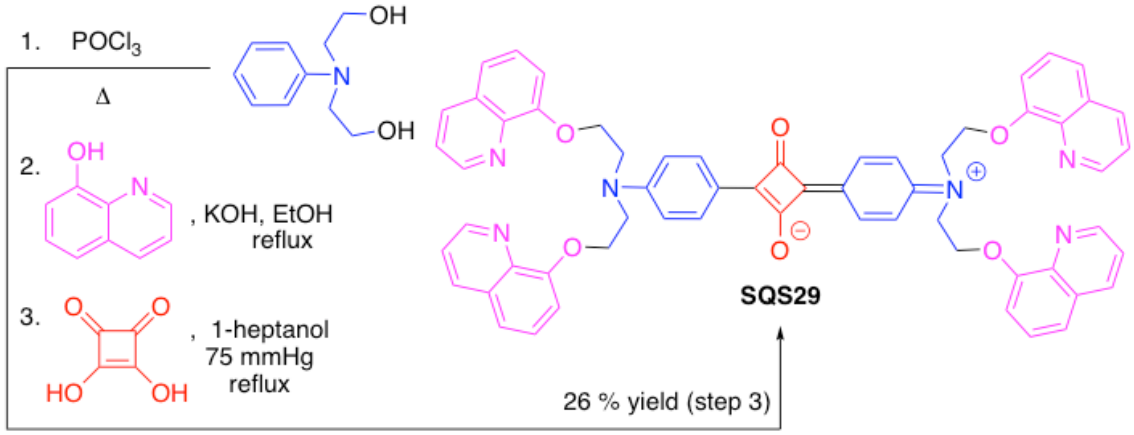

Scheme 11. Synthesis of symmetric quinoline-containing Hg^{2+}-selective **SQS29** [97].

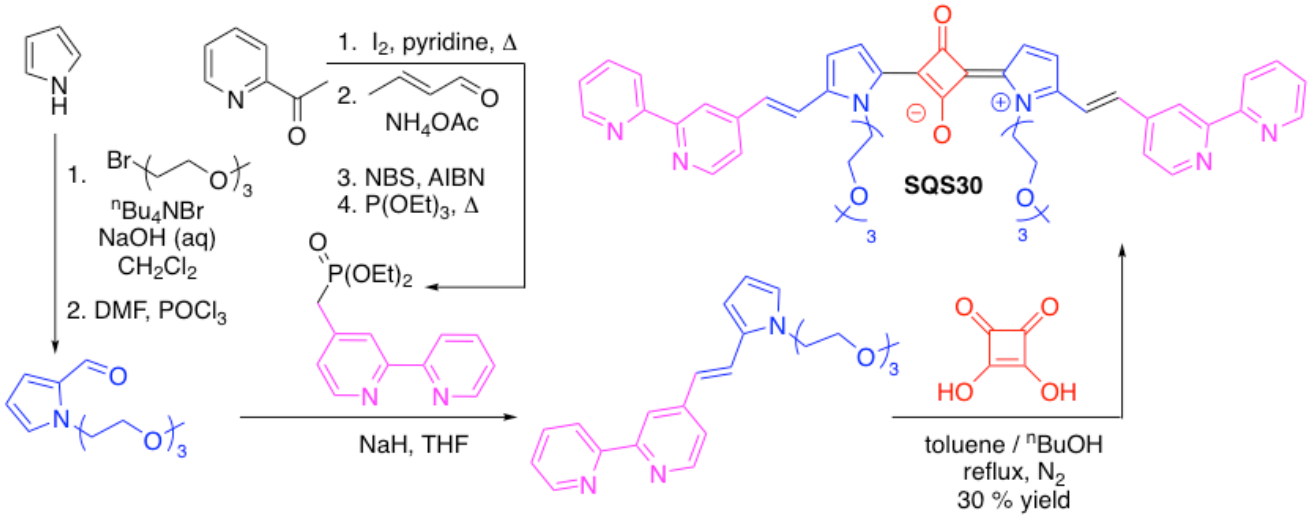

Scheme 12. Synthesis of bipyridyl-containing **SQS30** [98] for metal ion recognition.

4. Squaraine Scaffolds with Acidic NH

By taking advantage of the fairly acidic nature of NH, a N-nucleophilic-based CO_2 sensor **SQS31** was introduced (Scheme 13). **SQS31** was synthesized in a fairly straightforward manner, starting with diethyl squarate [99]. In the presence of less than 5 equiv. of tetrabutylammonium fluoride (TBAF, with F^- acting as a base), the yellow-colored **SQS31** solution in DMSO ($\lambda_{ab}{}^{max}$ = 445 nm) changed to a purple-colored solution ($\lambda_{ab}{}^{max}$ = 525 nm) **SQS31-1**. When an excess of F^- was used (ca. 20 equiv. of TBAF), a green solution ($\lambda_{ab}{}^{max}$ = 655 nm), attributed to the delocalized di-anion **SQS31-2**, was obtained. Although other halides did not deprotonate **SQS31** (due to low/non-existent basicity), NH_4OAc was able to induce similar changes in the absorption spectra of **SQS31** (both qualitatively and quantitatively).

Arguably, by adjusting the electronic demands of the substituents on the squaraine core, the acidity of the NH could be modulated to yield sensors towards various bases.

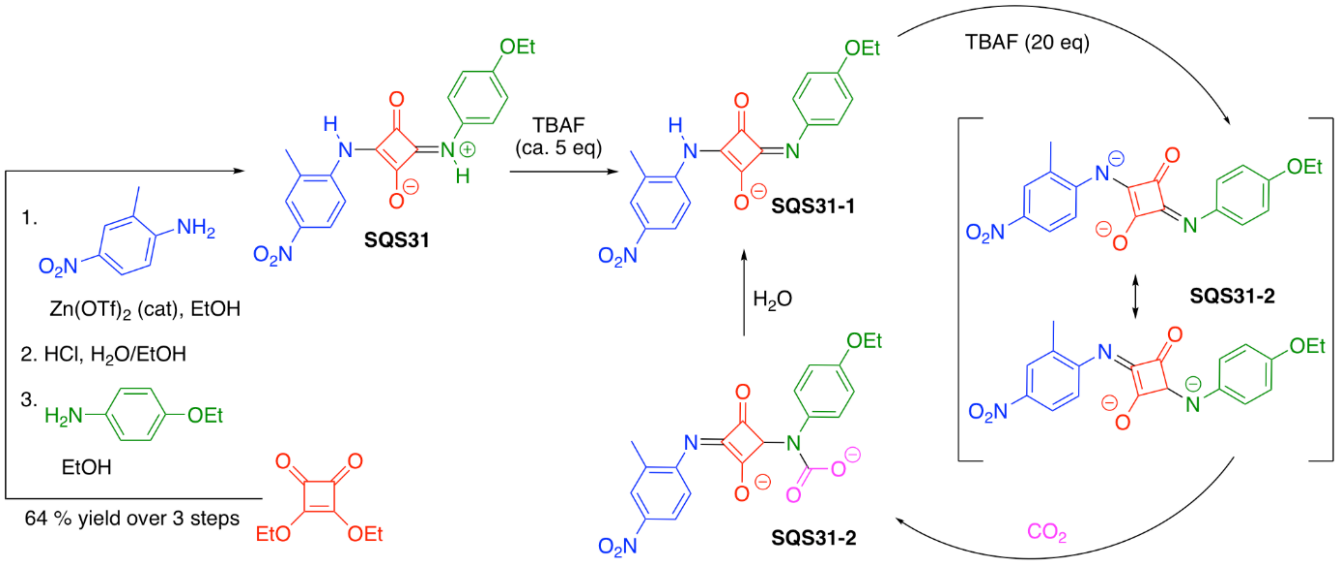

Scheme 13. Synthesis of **SQS31** [99], and CO_2 sensing cycle induced by F^-.

When a solution of **SQS31-2** was treated with various amounts of CO_2, a blue shift in the absorption maximum, from 655 nm to 525 nm, was observed (Scheme 13, a rapid conversion of **SQS31-3** to **SQS31** was assumed). The limit of CO_2 detection was estimated to be about 0.64 μM. Importantly, the response of **SQS31-1** to CO_2 appeared to be fairly fast and reversible, which allowed for 30 cycles of switching between 655 nm (**SQS31-1**) and 525 nm (**SQS31-2**), via alternating additions of TBAF and CO_2. Overall, a naked-eye detection of CO_2 and F^- by **SQS31** was realized.

Subsequently, a more elaborate sensor, **SQS32**, where a vinylic amine was conjugated to the squaraine scaffold, was synthesized, following a two-step procedure, using a dimethylaniline-containing semisquaraine as the starting material (Scheme 14) [100]. Upon the treatment of **SQS32** with TBAF, intermediate **SQS32-1** ($\lambda_{ab}{}^{max}$ = 405 nm) was produced, whose spectral properties differed drastically from **SQS32** ($\lambda_{ab}{}^{max}$ = 539 nm). This process (Scheme 14) was accompanied by the color change from pink (**SQS32**) to yellow (**SQS32-1**), which provided the naked-eye detection of F^- (similarly to those observed for **SQS31**; Scheme 13). Changes were also noted in the emission spectra of **SQS32** in the presence of F^-; the emission intensity of **SQS32** ($\lambda_{em}{}^{max}$ = 611 nm; red-colored solution under 365 nm UV lamp irradiation) decreased as a function of increasing concentration of F^-, with a concomitant increase in **SQS32**'s emission intensity ($\lambda_{em}{}^{max}$ = 485 nm; green-colored solution under 365 nm UV lamp irradiation). Not surprisingly, other halides (i.e., non-basic Cl^-, Br^-, and I^-) did not induce any formation of **SQS32-1**, as judged by the lack of any changes in the absorption and emission spectra of **SQS32** in the presence of these anions [100]. However, it is of interest to note that, similarly to **SQS31** (Scheme 14), NH_4OAc was also able to produce a deprotonated intermediate **SQS32-1**, albeit less efficiently than TBAF (a decrease of about 2.5-fold was determined, based on the changes in both the absorption and emission spectra).

When **SQS32-1** was exposed to CO_2, a conversion to **SQS32** was noted in accordance with the changes in the absorption and emission maxima, and the respective intensities [100]. Based on DFT calculations, it was proposed that **SQS32-1** was likely to act as a base to generate HO^-, which, in turn, would lead to the formation of HCO_3^- upon the reaction with CO_2 (Scheme 14). This was contrary to a more conventional interaction between **SQS32-1** and CO_2, which would have led to an unstable intermediate **SQS32-2,** with subsequent generation of HCO_3^- and **SQS32** (Scheme 14).

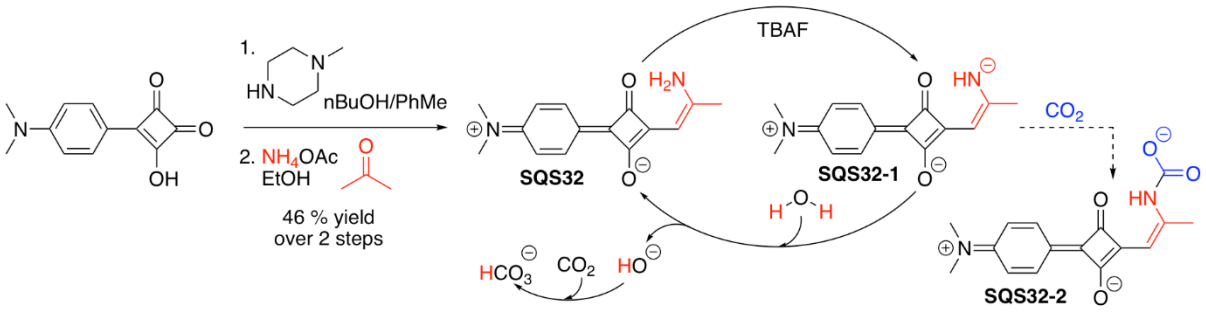

Scheme 14. NH_2-containing CO_2 **SQS32** [100]. Dotted arrow indicates a possible, traditionally assumed route to carbamate formation.

Overall, the results of these studies indicated that readily accessible squaraine-based sensors could be used for the visual and spectroscopic detection of CO_2. In view of the tunable acidity of NH, the design of other multi-analyte squaraine-based platforms should be possible.

5. Electrophilicity of Squaraine Ring's Carbon as Key Element in "Turn-Off" and "Turn-On" Sensing Paradigms

A number of chemosensors operate in the "turn-OFF" regime when a nucleophilic attack on the electrophilic center of the chemosensor disrupts the conjugation system, and, as such, this leads to a demise of low-energy absorption and emission bands [101,102]. The addition of the nucleophile to the squaraine core produced non-emissive species, while the addition of appropriate analytes led to the elimination of the nucleophile, restored the squaraine conjugation, and regenerated the original photophysical properties (Figure 6A). Squaraine-based chemodosimeters that are responsive to various nucleophilic analytes have been reported, including thiols (Figure 6B) [103–106], nitrogen-containing nucleophiles, such as amines and hydrazine (Figure 6C) [107], as well as cyanide ion (Figure 6D) [108,109]. It should be noted that thiol and hydrazine additions to squaraines could typically be reversed by the addition of thiophilic metal ions or aldehydes, respectively. In some instances, differentiation among similar Nu and X species (Figure 6A) could be achieved by the application of pattern-based recognition methods [110,111]. This approach was exemplified by **SQS33**, which was able to differentiate the effects of five thiols (e.g., propane thiol, 3-mercaptopropionic acid, naphthalene-2-thio, 2,3-dimercaptopropanol, and 2-acetylamino-3-mercaptopropionic acid methyl ester) and five metal ions (e.g., Hg^{2+}, Pd^{2+}, Cu^{2+}, Fe^{2+}, and Ni^{2+}) [103]. In general, the addition of CN^- to squaraine's electrophilic four-membered ring is not reversible.

Structurally, these sensors (Figure 6B–D) range from rather generic (**SQS33**) and relatively simple (**SQS34**) to more elaborate sensors, such as **SQS35** and **SQS36**, which possess moieties for metal ion recognition or aggregation-induced emission capabilities, respectively. It should also be kept in mind that, often, selectivity towards a certain analyte is determined by using a set of related species, i.e., the sensor's selectivity towards a specific ion will be assessed using a series of related or relevant ions. As such, sensors might be simply "branded" for a specific class of analytes. This might potentially limit further studies into the expanded scope of other analytes for this sensor. From the sensor's utility point of view, however, it might be advantageous to use one sensor for the detection of analytes that belong to different classes of compounds by simply adjusting the media in which the detection process is taking place; for example, simply by manipulating the nature of the media, **SQS35** (Figure 6) showed excellent selectivity towards various nucleophilic species, such as thiols (CH_3CN/H_2O 1/4, *v/v*; buffered at pH 6 (10 mM MES)) [105]. Under the aforementioned condition, **SQS35** did not optically respond to the presence of CN^-. However, in neat CH_3CN, **SQS35** exhibited excellent selectivity towards CN^- over other nucleophilic anions, such as F^- and AcO^- [108]. Yet, it should be noted that **SQS35**

in CH_3CN also optically responded to the presence of metal ions, such as Hg^{2+}, Fe^{3+}, and Cu^{2+} [58].

A few additional interesting and squaraine-unique cases, in regards to nucleophilic addition to squaraine's four-membered ring, are detailed below.

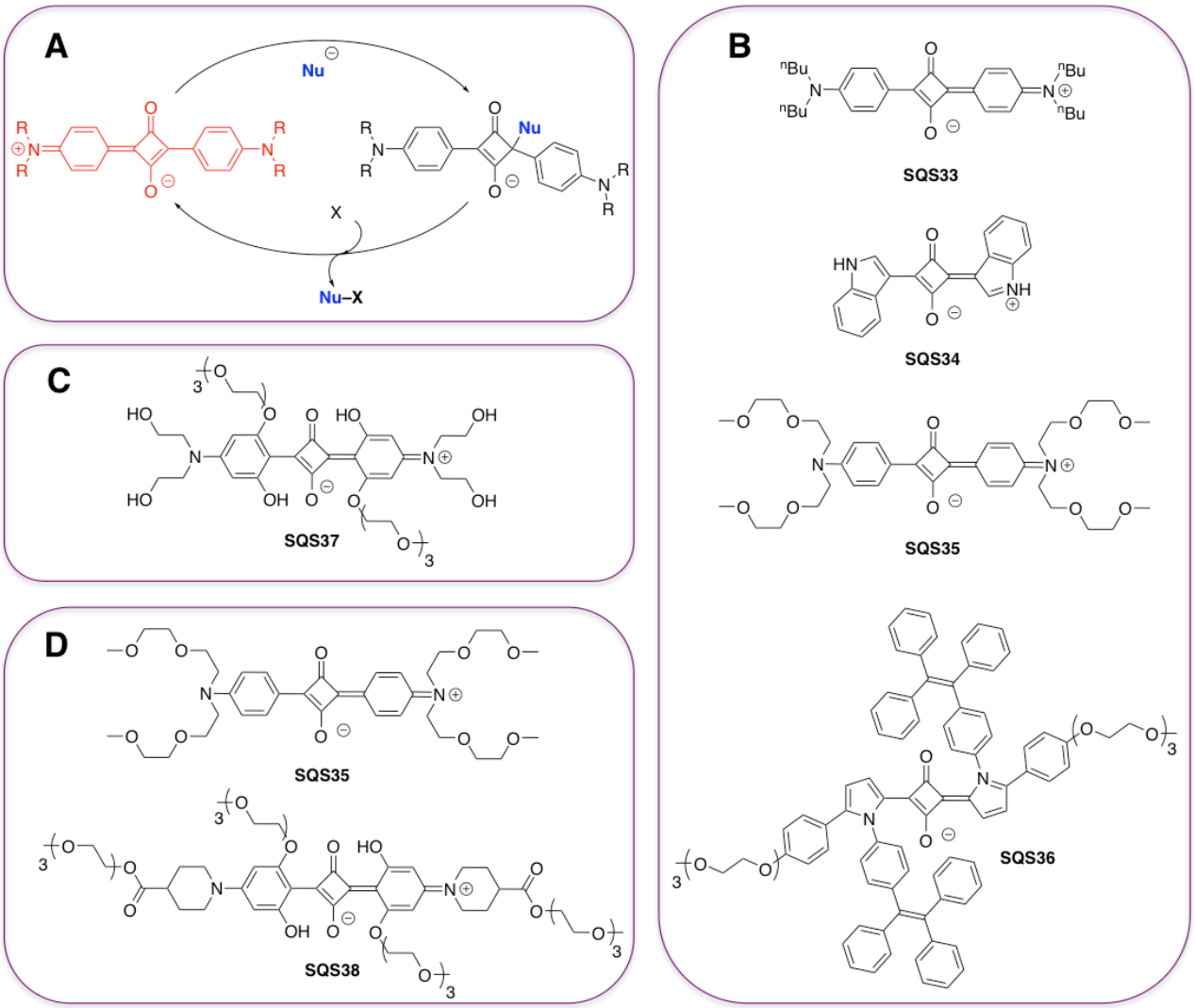

Figure 6. Some examples of nucleophile-sensitive SQSs. ON–OFF–ON relay of nucleophile-specific chemodosimeter (**A**). Representative structures of the following SQSs that showed sensitivity towards thiols (**B**): **SQS33** [103], **SQS34** [104], **SQS35** [105], **SQS36** [106]; the following to hydrazine and amines (**C**): **SQS37** [107]); the following to cyanide ion (**D**): **SQS38** [108], **SQS39** [109]).

5.1. Nucleophilic Addition as a Tool for Controlling Energy Transfer

It was shown (Section 4) that when an acidic NH is present, F^- (in the form of TBAF, for example) could act as a base and elicit the formation of a nucleophilic nitrogen center as a viable precursor for CO_2 sensing (Schemes 13 and 14). However, in the absence of acidic NH (i.e., C arene-type squaraines; Figure 1), F^- might be expected to act as a nucleophile towards the electrophilic carbon on the squaraine ring. Indeed, squaraines, which are obtained via Nu^C addition to squaric acid or its congeners (Schemes 1 and 2), could serve as "turn-OFF" sensors for the F^- nucleophile, which could attack the electrophilic center of the squaraine ring [112]. The squaraine scaffold was decorated with an additional fluorophore, thus coupling an energy transfer process (i.e., Förster resonance energy transfer—FRET) with nucleophilic sensing (Scheme 15). **SQS39**, which was synthesized in just five steps,

was specifically designed as a nucleophile-regulated FRET-ON to FRET-OFF sensor. **SQS39** exhibited the following two absorption maxima: 400 nm, which corresponded to the naphthalimide unit (Scheme 15, moiety shown in blue), and 659 nm, which corresponded to the squaraine unit (Scheme 15, moiety shown in red). Upon excitation of the naphthalimide unit (λ_{ex} = 400 nm), FRET to the squaraine unit (λ_{em} = 667 nm) was observed with over 90% efficiency (in CH_3CN, and in the CH_3CN/H_2O mixture (9/1, *v*/*v*)). As expected, upon titration of **SQS39** (10 μM) with F^- (2 μM–1.2 mM, which acted as a nucleophile), the intensity of the band associated with the squaraine unit decreased, due to disruption of the conjugated system. Not surprisingly, F^- did not have any impact on the naphthalimide, since there were no viable electrophilic centers on this chromophoric unit. The intensity of emission at 667 nm (associated with squaraine) was decreasing, while the emission at 537 nm (associated with naphthalimide) was increasing, as a function of the added F^-, which resulted in ratiometric FRET-based sensing. Since a qualitatively similar ratiometric response for **SQS39** was noted upon addition of CN^-, it could be argued that **SQS39** (and other related squaraine-based multi-dye systems) could be used for the detection of other nucleophilic species.

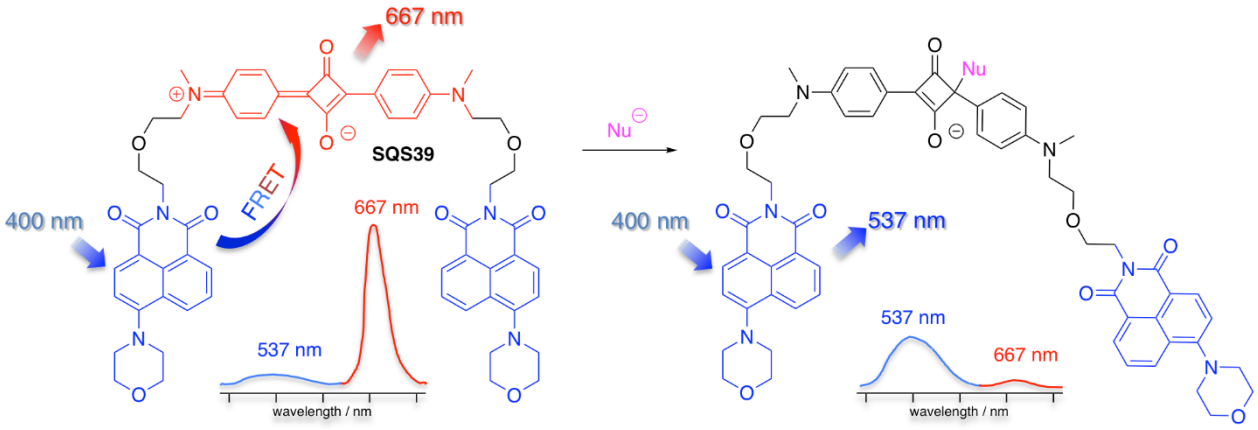

Scheme 15. FRET-based sensor **SQS39** for nucleophilic anions [112]. Nu = F^- or CN^-. Fluorescence spectra qualitatively demonstrate changes in the emission intensities at 537 nm (naphthalimide moiety, shown in blue) and at 667 nm (squaraine moiety, shown in red) before (**left**) and after (**right**) exposure of **SQS39** to Nu.

5.2. Nucleophile-Induced Skeletal Rearrangement

Several phosphines, e.g., P^nBu_3, $P(NMe_2)_3$, and P(p-MeO-C_6H_4), were shown to be efficient nucleophiles towards an electrophilic carbon of the squaraine core of **SQS40** (Scheme 16A) [113]. Similarly to the nucleophilic addition of thiols to squaraines, the addition of P(III)-nucleophiles also led to an emission "turn-OFF" response. The P-containing adducts have photophysical characteristics that are drastically different from the initial squaraines, i.e., green–blue color of the squaraine **SQS40** faded away in the presence of the phosphines, and produced a yellow product, **SQS40-1**, as was evident by the disappearance of the absorption band at 656 nm. Notably, when a bulkier $P(p\text{-}MeOC_6H_4)_3$ was used, the nucleophilic addition was found to be reversible, with the P-adduct being favored by lower temperatures. A temperature-dependent NMR study revealed the reversible nature of this P-nucleophilic addition to the squaraine. Interestingly, contrary to the addition of thiols to squaraines, where the association is typically favored by higher temperatures, in the case of phosphine addition, the equilibrium was heavily shifted towards the P-adduct at lower temperatures [113]. Thus, thermochromic applications might be exploited using these zwitterionic P-containing adducts.

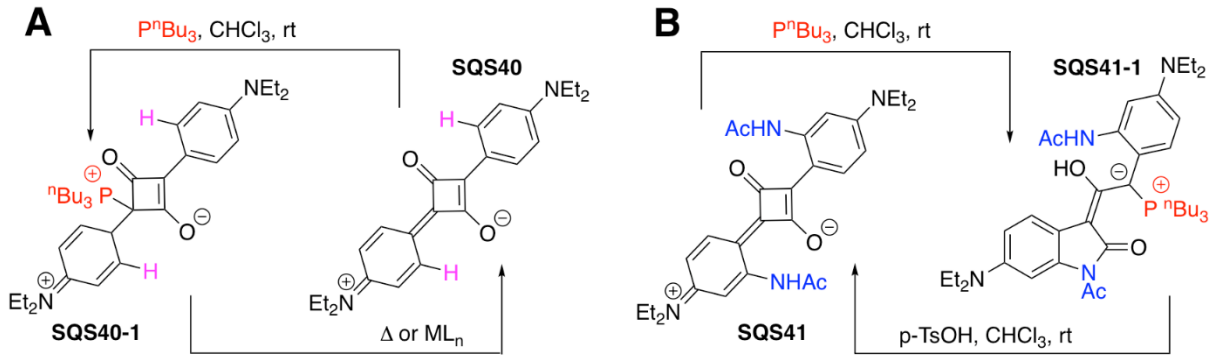

Scheme 16. Representative examples of relays that feature phosphine additions to squaraine scaffolds (**A**): **SQS40** [113] and (**B**): **SQS41** [114].

Furthermore, in view of the ease of the synthesis and purification/isolation (pure products were obtained by vapor–vapor crystallization) of these P-containing zwitterionic compounds, e.g., **SQS40-1** (Scheme 16A), the use of these compounds as sensors for transition metals was explored. Specifically, a number of transition metal ions, such as Pd^{2+}, Rh^{+}, Ag^{+}, Au^{3+}, as well as Cu^{+} and Cu^{2+}, were able to induce phosphine elimination and restore the squaraine's structure **SQS40** (confirmed by the appearance of the characteristic color associated with **SQS40**, $\lambda_{ab}{}^{max}$ = 656 nm). On the other hand, Ni^{2+}, Fe^{3+}, Ti^{3+}, and Ti^{4+} failed to eliminate the P-containing moiety from **SQS40-1**, as was evident from the persistent yellow color of the solution.

In a subsequent study, it was found that the presence of certain substituents (i.e., OH, NHAc, NHTs, and NHBoc) in the ortho-position of the aromatic rings could induce a cascade of reactions, following P-nucleophilic addition to the squaraine ring, leading to the formation of furanone or oxindole scaffolds (Scheme 16B) [114]. Specifically, P^{n}Bu$_3$ addition to NHAc-containing squaraine **SQS41** produced oxindole **SQS41-1** (Scheme 16B). Similarly to previous PR_3 additions to squaraines, P^{n}Bu$_3$ addition to **SQS41** was accompanied by a change in color from blue to colorless, thus resulting in a "turn-OFF" sensing mechanism. Importantly, the reversed process, i.e., reformation of the squaraine core, was achieved by the addition of the acid to **SQS41-1** to restore **SQS41**; thus, a "turn-ON" pH-sensing mechanism was realized (Scheme 16B).

6. Chemo-Uncaging Strategies for Sensing

Although squaraine-based sensors that rely on a nucleophilic attack on the electrophilic carbon of the squaraine ring have been widely utilized, it could be argued that a "turn-OFF" type of response might not be optimal for some applications, especially those related to biological environments. Therefore, developing alternative strategies that yield a "turn-ON" type of squaraine sensor would be advantageous. In order to explore this avenue, the squaraine ring's susceptibility to nucleophilic attacks must be addressed. To this end, several strategies to protect squaraines from nucleophilic attack have been developed. Specifically, threading squaraine through a macrocyclic scaffold, thus generating a rotaxane-type system (Figure 7A), proved to be a viable approach for not only making squaraines chemically inert to nucleophilic insults, but also preventing the aggregation of squaraine dyes, thus preserving the desired photophysical characteristics of the monomeric state [115]. As such, these squaraine-threaded rotaxane systems have been demonstrated to be useful for various bioimaging applications [116–118]. However, additional synthetic steps are required for the synthesis of the macrocycle, as well as the synthesis of the rotaxane, which might decrease the synthetic accessibility of the desired squaraine-based chemosensor.

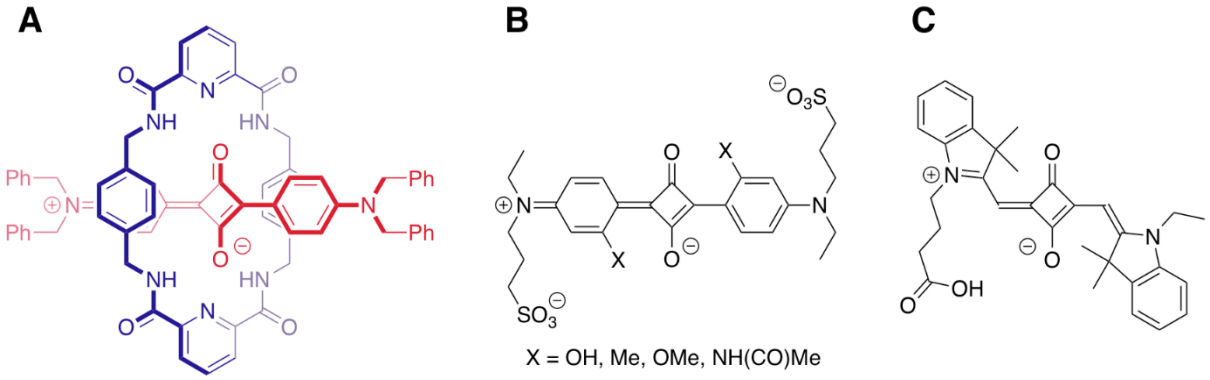

Figure 7. Squaraine dyes with reduced reactivity towards thiol nucleophilic attack on the squaraine's electrophilic center. (**A**): a representative example of squaraine rotaxane [116]; (**B**): ortho-substituted squaraines [119]; (**C**): symmetric arylidene squaraine [120].

Thus, as a complementary approach, chemical modification of the squaraine, to prevent nucleophilic attack on the four-membered ring, was also explored. Arguably, simply incorporating substituents into the ortho-position of the aromatic substituents on the squaraine ring could reduce the electrophilicity of the squaraine's ring. It appeared that an intricate balance between electronic and steric factors could modulate the rate of thiol addition to the electrophilic center on the squaraine ring (Figure 7B) [119]. Importantly, the presence of a single OH group on each of the aromatic moieties was shown to be sufficient for almost completely inhibiting the nucleophilic attack of N-acetyl cysteine.

Additionally, it was shown that squaraines that feature the arylidene-type moiety (Figure 7C) are not susceptible to nucleophilic attack by dimercaprol, i.e., aliphatic dithiol [120]. This type of squaraine dye, both the symmetric and non-symmetric versions, could be easily obtained from CH-active nucleophiles (i.e., Nu^C-H; Schemes 1 and 2).

It has long been established that the incorporation of an electron-withdrawing moiety on a chromophoric scaffold could quench the fluorophore emission, and, thus, yield the OFF-state of the fluorophore. Assuming that the removal of that moiety, a process that could also be referred to as either deprotection or uncaging, does not affect the structural integrity of the fluorophore, the ON-state could be realized [121,122]. In particular, the 2,4-dinitrobenzenesulfonyl group, along with the 4-nitrobenzylsulfonyl and pentafluorobenzenesulfonyl groups, when conjugated onto several fluorophoric scaffolds, such as coumarin, rhodamine, and crystal violet, were shown to efficiently quench the emission of the fluorophore, thus giving the OFF-state of the sensor [123,124].

The sensor **SQS42**, bearing the 2,4-dinitrobenzenesulfonyl moiety as the caging element, was obtained in four linear steps with a 13% overall yield (Scheme 17). Spectroscopically, the caged sensor **SQS42** and the related parent **SQS42-1** exhibited the same absorption and emission maxima ($\lambda_{ab}{}^{max}$ = 635 nm, $\lambda_{em}{}^{max}$ = 656 nm), yet the quantum yields' difference was over 30-fold (0.006 and 0.203, respectively) [125].

However, when low-emission **SQS42** was treated with increasing amounts of Cys, highly emissive **SQS41-1** was produced. Notably, higher concentrations of thiols led to a decrease in the absorption of the squaraine chromophore ($\lambda_{ab}{}^{max}$ = 635 nm), due to nucleophilic attack on the four-membered ring electrophilic center [125].

In order to inhibit the competing reaction, **SQS43** was introduced (Scheme 17) [126]. The arylidene moiety (shown in red) provided enhanced stability towards the nucleophilic attack (in line with model squaraine; see Figure 6C), whereas the glycol tethered carbohydrate moiety (shown in pink) was introduced to enhance the solubility in aqueous media. The thiolate attack was shown to be much more facile at the electrophilic center of the 2,4-dinitrobenzenesulfonyl moiety, rather than at the squaraine's core. No decrease in either the absorption or fluorescent emission intensities was noted, even when excess amounts of thiol were used [126].

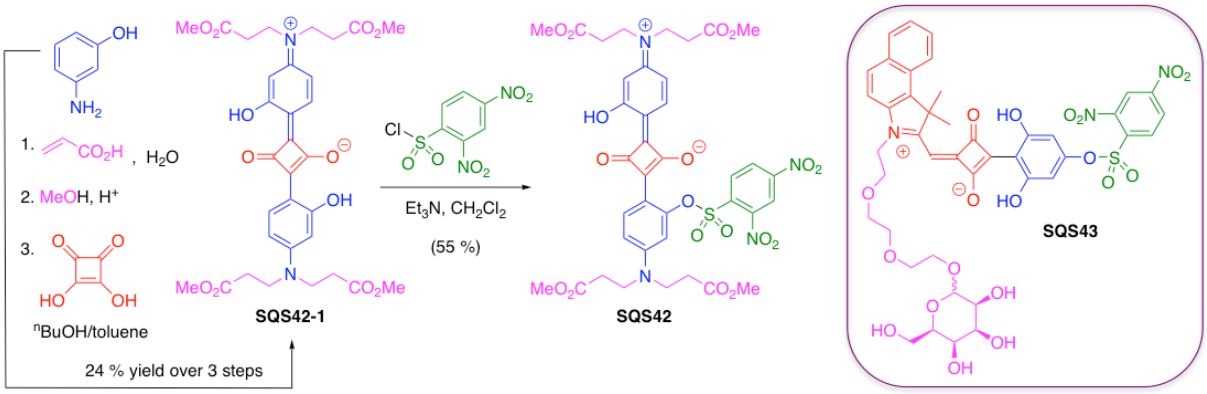

Scheme 17. Synthesis of caged **SQS42** [125] and structure of water-soluble, caged **SQS43** [126].

It is also important to note that, in aqueous media, around neutral pH, it is possible to differentiate between aromatic and aliphatic thiols, since aromatic thiolates are better nucleophiles than aliphatic thiolates (due to the higher acidity of the S–H bond, and, as a result, more facile generation of the thiolate anion). Therefore, chemical uncaging of a probe using aromatic thiols proceeds significantly faster compared to aliphatic thiols [127,128]. Thus, **SQS43** could be turned into an aromatic thiol-specific probe by simply adjusting the pH of the media [126].

Recently, a thio-squaraine-specific Hg sensor, **SQS44,** was introduced, and it featured a Hg^{2+}-induced S-to-O- "uncaging" optical sensing mechanism (Scheme 18) [129]. This approach took advantage of the well-established ability of Lawesson's reagent to convert carbonyl groups into thiocarbonyl-containing ones [130], and the fact that Hg^{2+} could trigger the reverse desulfurization reaction with a high degree of functional group tolerance [8]. Symmetric squaraine **SQS44-1** was synthesized following general protocols, and the subsequent incorporation of sulfur atoms on the squaraine's four-membered ring was achieved using Lawesson's reagent under standard conditions [130], to give **SQS44** (Scheme 18).

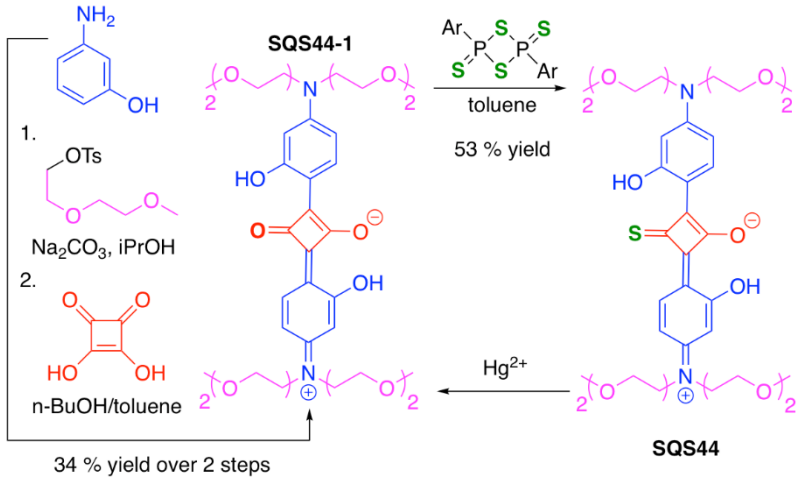

Scheme 18. Synthesis of sulfur-containing **SQS44** and Hg^{2+}-triggered uncaging of **SQS44** [129].

Due to the heavy atom effect, i.e., S for O substitution, the emission of sulfur-containing **SQS44** appeared to be significantly decreased compared to the oxygen-containing analogue **SQS44-1**; for example, the quantum yields for **SQS44** and **SQS44-1** were 0.163 and 0.647, respectively. However, in the presence of increasing amounts of $Hg(NO_3)_2$, a substantial increase in emission intensity ($\lambda_{em}{}^{max}$ = 657 nm) was noted, thus yielding a "turn-ON" sensor [129]. **SQS44** operated in a relatively wide pH range (pH 3.0–7.0, which is suitable

for various biological systems), and provided an acceptable detection limit of Hg^{2+} (estimated at 1.2 nM). Remarkably, other thiophilic metal ions, such as Pb^{2+}, Cd^{2+}, and Ag^{+}, failed to induce any appreciable changes in the emission spectra. Furthermore, due to its relatively low cytotoxicity and acceptable aqueous solubility, **SQS44** was subjected to in vitro (HeLa cell) and in vivo (zebra fish) fluorescence imaging studies. In both environments, **SQS44** showed good stability and appreciable Hg^{2+}-sensing capability [129], which makes it a viable and potentially useful near-IR probe for fluorescence imaging of various biological systems.

7. Squaraine–Metal Scaffold for Sensing

Molecular platforms with multiplexing capabilities are of interest. Arguably, in view of the facile and modular synthetic access to structurally and functionally diverse structures, including post-modification options, squaraine dyes might be among the most versatile scaffolds to design and synthesize sensors for multi-analyte recognition.

A dipicolylamine-containing squaraine, **SQS45** (sensing ability beyond interaction with Zn^{2+} is yet to be established), which was prepared following standard protocols, was complexed with Zn^{2+} to give squaraine scaffold **SQS46** that showed the ability to sense CO_2, picric acid, and phosphates (Scheme 19). It should be noted that **SQS46** was not isolated, but rather used as prepared, i.e., CH_3CN with excess $Zn(ClO_4)_2$ (last step in Scheme 19). In all the cases, coordination of the oxygen atom(s) of the analytes to the Zn center of **SQS46** modulated the photophysical properties of the sensing scaffold [131].

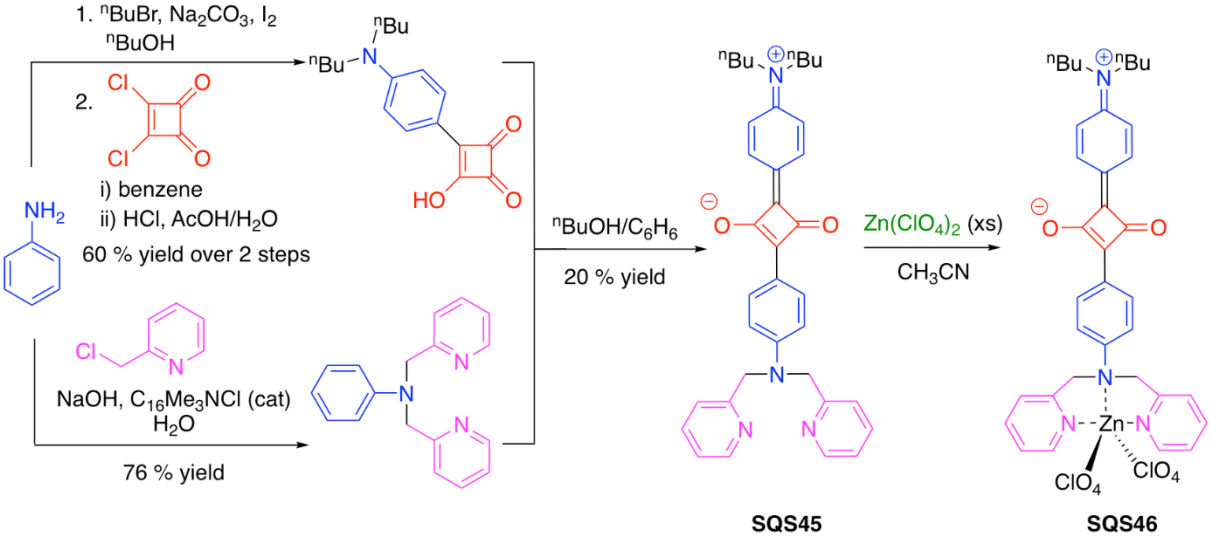

Scheme 19. Synthesis of squaraine-based Zn-containing sensing scaffold **SQS46** for anion and molecular recognition [131].

When an acetonitrile solution of **SQS46** (containing ca. 1% of water, *v/v*) was purged with CO_2, a color change from violet to blue was noted, along with a decrease in the 584 nm absorption band, and an increase in the absorption band at 633 nm. Although the emission of **SQS46** in CH_3CN is fairly low, in the presence of increasing amounts of CO_2, a "turn-ON" response, with $\lambda_{em}{}^{max}$ = 659 nm, was observed [131]. ^{13}C NMR investigation revealed the presence of a carbonate anion, which indicated that CO_2 sensing by **SQS46** was conducted in the form of the carbonate. In fact, when **SQS46** was treated with carbonate ions, spectroscopic and visual changes in the **SQS46** solution, which were similar (yet more rapid) to those observed upon the purging with CO_2, were observed. Furthermore, drastically smaller changes, in both the absorption and emission spectra (as well as no color change in the **SQS46** solution), were observed in the absence of water in the system, upon prolonged purging with CO_2. In addition, it was reported, albeit with little detail, that the bound carbonate could be released in the presence of Ca^{2+}. Thus, in principle, an even

more elaborate sensing platform could be realized, which will implement a regeneration of **SQS46**.

Next, interactions between **SQS46** and various phosphate anions were explored [131]. **SQS46** allowed for a naked-eye differentiation between cyclic and linear phosphates, including GMP and c-GMP. Specifically, the absorption maximum of **SQS46** ($\lambda_{ab}{}^{max}$ = 584 nm; purple-colored solution) was red-shifted to 615 nm (blue-colored solution) in the presence of cyclic phosphates, and further red-shifted to 633 nm (light-blue-colored solution) in the presence of linear phosphates. The changes in the emission spectra of **SQS46** were also pronounced. Similarly to the aforementioned CO_2/carbonate case, a "turn-ON" response was noted when **SQS46** was titrated with phosphates. Similar levels of emission enhancements were observed in the cases of both cyclic and linear phosphates (i.e., a ca. 8–9-fold increase in emission intensity in the presence of 6–7 equiv. of phosphates), and, in both cases, the ppm levels of the detections were estimated. However, the emission maxima were distinct enough to assure differentiation between cyclic and linear phosphates; for **SQS46**–c-GMP, the $\lambda_{em}{}^{max}$ was 644 nm, and for **SQS46**–GMP, the $\lambda_{em}{}^{max}$ was 659 nm.

In addition to ionic recognition, **SQS46** showed appreciable capability in molecular sensing [131]. Specifically, the purple-colored (λ_{ab} = 584 nm) solution of **SQS46** in acetonitrile changed to green (λ_{ab} = 644 nm) upon addition of an aqueous solution of picric acid. Thus, a naked-eye determination of an explosive was achieved. **SQS46** also acted as a fluorescent "turn-ON" sensor for picric acid, as a gradual increase in the emission intensity at 644 nm was noted upon titration of **SQS46** solution with picric acid (up to ca. 10-fold emission enhancement was noted in the presence of 15 equiv. of picric acid), and provided a detection limit of 3 ppm. Furthermore, ca. 6.5-fold selectivity over other nitrophenols (e.g., 2-nitro/3-nitro/4-nitro-phenols) was noted.

8. Conclusions

The tunable photophysical properties and synthetic accessibility of squaraine dyes make them one of the most versatile, privileged chromophoric and fluorophoric scaffolds, which are almost ideal for designing and synthesizing various optical chemosensors. This review illustrated a plethora of approaches towards squaraine-based chemosensors that allow for "turn-ON", "turn-OFF", and relay-type sensing modes for the detection of various ionic and molecular analytes. In addition, non-symmetric squaraine-based sensors allow for further modulation of photophysical properties and solubilities, as well as providing additional possibilities for the conjugation and immobilization of these sensors on other platforms.

Decorating squaraine dyes with various structurally and functionally diverse moieties has produced a number of chemosensing scaffolds with optical responses that cover a wide spectra window in the presence of various types of ionic and molecular analytes (Table 1). However, as exemplified by a number of accounts, the sensing ability and selectivity of SQSs appear to also be dependent on the media used. Hence, it might be advantageous to evaluate sensors' analyte recognition capabilities in various types of media, i.e., in regards to the nature of the solvents and/or composition for mixed solvent systems, such as aqueous/organic solvents. Importantly, developing and utilizing standard sets of conditions that would be used for screening specific analytes should allow for meaningful comparisons of the sensing capabilities of various SQSs.

Although the post-functionalization of squaraine scaffolds is possible, most synthetic approaches rely on the condensation of various C/N-nucleophiles, with squaric acid (or its congeners) as the last step in assembling the squaraine. Since the condensation step is performed under relatively mild conditions, many functional groups and structural motifs are tolerated. As such, the diversity of squaraine-based chemosensors, and, hence, the selectivity and sensitivity towards analytes, is only limited by the accessibility of the C/N-nucleophilic components and the researchers' imagination.

Table 1. A list of SQSs and their recognition motifs for sensing of various analytes.

Recognition Motif	SQS#	Analyte	Refs.
crown ether			
	SQS1	Li^+	[53]
	SQS2	Li^+, Na^+	[53]
	SQS3	Ba^{2+}, Pb^{2+}, Cu^{2+}, Fe^{3+}, Hg^{2+}	[58]
	SQS4	Mg^{2+}, Ba^{2+}	[59]
	SQS5	–	[60]
	SQS6	Li^+	[61]
	SQS7	Na^+	[62]
	SQS8	Hg^{2+}	[63]
	SQS9	Hg^{2+}, Ag^+, Fe^{3+}, Cu^{2+}	[58,66]
	SQS10	Pb^{2+}, Cu^{2+}	[67]
podand			
	SQS11	Ca^{2+}	[71]
	SQS12	Ca^{2+}, Mg^{2+}	[72]
	SQS13	Ca^{2+}, Mg^{2+}	[72]
	SQS14	Ca^{2+}, Mg^{2+}	[72]
	SQS15	Hg^{2+}	[74]
	SQS16	Hg^{2+}	[74]
	SQS17	Hg^{2+}	[75]
	SQS18	Hg^{2+}	[76]
	SQS19	Hg^{2+}	[77]
	SQS20	Hg^{2+}	[78]
	SQS21	Hg^{2+}	[79]
	SQS22	Hg^{2+}, Cu^{2+}, Fe^{3+}	[80]
	SQS23	Hg^{2+}, Cys, Hcys, GSH	[81]
	SQS24	Hg^{2+}, Ag^+, Cys, His, Trp	[82]
tetracarboxylate			
	SQS25	Ca^{2+}	[86]
nitrogen-containing heterocycle			
	SQS26	Hg^{2+}	[94]
	SQS27	Cu^{2+}	[96]
	SQS28	Cu^{2+}	[96]
	SQS29	Hg^{2+}	[97]
	SQS30	Zn^{2+}, Cd^{2+}, Cu^{2+}, Co^{2+}, Ni^{2+}, Ag^+	[98]
acidic NH			
	SQS31	F^-, CO_2	[99]
	SQS32	F^-, CO_2	[100]
squaraine-ring as electrophile			
	SQS33	propane-1-thiol, 3-mercapto-propionic acid, 2-acetylamino-3-mercapto-propionic acid methyl ester, 2,3-dimercapto-propane-1-ol, naphthalene-2-thiol; Pd^{2+}, Hg^{2+}, Ni^{2+}, Cu^{2+}, Fe^{2+}	[103]
	SQS34	4-acetamidothiophenol, N-acetyl-L-Cys, L-Cys methyl ether, L-Cys, 2-(dimethylamino)ethanethiol; Hg^{2+}	[104]
	SQS35	propanethiol, Cys, Cys-Gly, GSH	[105]
		CN^-	[108]
	SQS36	Cys, GSH	[106]

Table 1. *Cont.*

Recognition Motif	SQS#	Analyte	Refs.
	SQS37	NH_2NH_2, HO^-, ethanolamine, methylamine, β-phenylethylamine; glyoxal, glutaric dialdehyde, propionaldehyde, pyridine-2-carboxaldehyde, formaldehyde, acetaldehyde	[107]
	SQS38	CN^-	[109]
	SQS39	F^-, CN^-	[112]
	SQS40	P^nBu_3, $PN(Me_2)_3$, $P(p\text{-}MeO\text{-}C_6H_4)_3$; Pd^{2+}, Rh^+, Ag^+, Au^{3+}, Cu^+, Cu^{2+}	[113]
	SQS41	P^nBu_3; TsOH	[114]
caging group			
	SQS42	Cys, Hcys	[125]
	SQS43	PhSH	[126]
	SQS44	Hg^{2+}	[129]
metal-containing scaffold			
	SQS45	Zn^{2+}	[131]
	SQS46	$CO_2/CO_3{}^{2-}$; GMP, c-GMP; picric acid	[131]

Author Contributions: Conceptualization, D.D.T. and S.V.D.; writing—original draft preparation, D.D.T. and S.V.D.; writing—review and editing, D.D.T. and S.V.D.; project administration, S.V.D.; funding acquisition, S.V.D. All authors have read and agreed to the published version of the manuscript.

Funding: This research was funded in part by National Institutes of Health, NIH, grant number 1R15GM135900-01.

Institutional Review Board Statement: Not applicable.

Informed Consent Statement: Not applicable.

Data Availability Statement: Not applicable.

Acknowledgments: The authors would like to thank NIH (1R15GM135900-01) and Texas Christian University (Department of Chemistry & Biochemistry) for financial support of our scholarly activities related to molecular probe and sensor development. D.D.T. is the recipient of the TCU-STAR fellowship.

Conflicts of Interest: The authors declare no conflict of interest.

References

1. He, J.; Jo, Y.J.; Sun, X.; Qiao, W.; Ok, J.; Kim, T.-I.; Li, Z. Squaraine dyes for photovoltaic and biomedical applications. *Adv. Funct. Mater.* **2021**, *31*, 2008201. [CrossRef]
2. Ilina, K.; MacCuaig, W.M.; Laramie, M.; Jeouty, J.N.; McNally, L.R.; Henary, M. Squaraine dyes: Molecular design for different applications and remaining challenges. *Bioconjugate Chem.* **2020**, *31*, 194–213. [CrossRef] [PubMed]
3. McEwen, J.J.; Wallace, K.J. Squaraine dyes in molecular recognition and self-assembly. *Chem. Commun.* **2009**, 6339–6351. [CrossRef] [PubMed]
4. Wu, J.; Kwon, B.; Liu, W.; Anslyn, E.V.; Wang, P.; Kim, J.S. Chromogenic/fluorogenic ensemble chemosensing systems. *Chem. Rev.* **2015**, *115*, 7893–7943. [CrossRef]
5. Sun, W.; Guo, S.; Hu, C.; Fan, J.; Peng, X. Recent development of chemosensors based on cyanine platform. *Chem. Rev.* **2016**, *116*, 7768–7817. [CrossRef]
6. Khopkar, S.; Shankarling, G. Synthesis, photophysical properties and applications of NIR absorbing unsymmetrical squaraines: A review. *Dyes Pigments* **2019**, *170*, 107645. [CrossRef]
7. Mako, T.L.; Racicot, J.M.; Levine, M. Supramolecular luminescent sensors. *Chem. Rev.* **2019**, *119*, 322–477. [CrossRef] [PubMed]

8. Kaur, K.; Saini, R.; Kumar, A.; Luxami, V.; Kaur, N.; Singh, P.; Kumar, S. Chemodosimeters: An approach for detection and estimation of biologically and medically relevant metal ions, anions and thiols. *Coord. Chem. Rev.* **2012**, *256*, 1992–2028. [CrossRef]
9. Mukkanti, A.; Periasamy, M. Methods of synthesis of cyclobutenediones. *ARKIVOC* **2005**, *11*, 48–77. [CrossRef]
10. Xia, G.; Wang, H. Squaraine dyes: The hierarchical synthesis and its application in optical detection. *J. Photochem. Photobiol. C* **2017**, *31*, 84–113. [CrossRef]
11. Hu, L.; Yan, Z.; Xu, H. Advances in synthesis and application of near-infrared absorbing squaraine dyes. *RSC Adv.* **2013**, *3*, 7667–7676. [CrossRef]
12. Sprenger, H.-E.; Ziegenbein, W. Cyclobutenediylium dyes. *Angew. Chem. Int. Ed.* **1968**, *7*, 530–535. [CrossRef]
13. Mayerhöffer, U.; Fimmel, B.; Würthner, F. Bright near-infrared fluorophores based on squaraines by unexpected halogen effects. *Angew. Chem. Int. Ed.* **2012**, *51*, 164–167. [CrossRef]
14. Wendling, L.A.; Koster, S.; Murray, J.E.; West, R. Syntheses and properties of 1,2- and 1,3-diquinocyclobutanediones. *J. Org. Chem.* **1997**, *42*, 1126–1130. [CrossRef]
15. Law, K.Y.; Bailey, F.C. Squaraine chemistry. Synthesis, characterization, and optical properties of a class of novel unsymmetrical squaraines: [4-(dimethylamino)phenyl](4′-methoxymethyl)squaraine and it derivatives. *J. Org. Chem.* **1992**, *57*, 3278–3286. [CrossRef]
16. Law, K.Y.; Bailey, F.C. Squaraine chemistry. A new approach to symmetrical and unsymmetrical protoconductive squaraines. Characterization and solid state properties of these materials. *Can. J. Chem.* **1993**, *71*, 494–505. [CrossRef]
17. Hamilton, D.G.; Lynch, D.E.; Smith, G. Synthesis and solid-state structure of the unsymmetrical squaraine dye 2-[4-(dibutylamino)-2-hydroxyphenyl]-4-[4-(dibutylamino)phenyl]-cyclobutenebis(ylium)-1,3-diolate. *Aust. J. Chem.* **1996**, *49*, 1339–1343. [CrossRef]
18. Piggot, P.M.T.; Hall, L.A.; White, A.J.P.; Williams, D.J. Attempted syntheses of lanthanide(III) complexes of the anisole and anilinosquarate ligands. *Inorg. Chem.* **2003**, *42*, 8344–8352. [CrossRef]
19. de Oliveira, V.E.; de Carvalho, G.S.; Yoshida, M.I.; Donnici, C.L.; Speziali, N.L.; Diniz, R.; de Oliveira, L.F.C. Bis(dicyanomethylene)squarate squaraines in their 1,2- and 1,3-forms: Synthesis, crystal structure and spectroscopic study of compounds containing alkali metals and tetrabutylammonium ions. *J. Mol. Struct.* **2009**, *936*, 239–249. [CrossRef]
20. Neuse, E.W.; Green, B.R. Dianilino derivatives of squaric acid. *J. Org. Chem.* **1974**, *39*, 3881–3887. [CrossRef]
21. Khopkar, S.; Deshpande, S.; Shankarling, G. Greener protocol for the synthesis of NIR fluorescent indolenine-based symmetrical squaraine colorants. *ACS Sustain. Chem. Eng.* **2018**, *6*, 10798–10805. [CrossRef]
22. Zappimbulso, N.; Capozzi, M.A.M.; Porcheddu, A.; Punzi, A. Solvent-free reactions for the synthesis of indolenine-based squaraines and croconaines: Comparison of thermal heating, mechanochemical milling, and IR irradiation. *ChemSusChem* **2021**, *14*, 1363–1369. [CrossRef]
23. Gauger, J.; Manecke, G. Kondensationsproducte der quadratsäure mit primären unde sekundären aminen, I. *Chem. Ber.* **1970**, *103*, 2696–2706. [CrossRef]
24. Keil, D.; Hartmann, H. Synthesis and characterization of a new class of unsymmetric squaraine dyes. *Dyes Pigments* **2001**, *49*, 161–179. [CrossRef]
25. Buchynskyy, A.; Kempin, U.; Vogel, S.; Hennig, L.; Findeisen, M.; Müller, D.; Giesa, S.; Knoll, H.; Welzel, P. Synthesis of fluorescent derivatives of the antibiotic moenomycin A. *Eur. J. Org. Chem.* **2002**, *2002*, 1149–1162. [CrossRef]
26. Kim, S.; Han, S. High performance squarylium dyes for high-tech use. *Color. Technol.* **2001**, *117*, 61–67. [CrossRef]
27. Xie, J.; Comeau, A.B.; Seto, T. Squaric acids: A new motif for designing inhibitors of protein tyrosine phosphatates. *Org. Lett.* **2004**, *6*, 83–86. [CrossRef]
28. López, C.; Vega, M.; Sanna, E.; Rotger, C.; Costa, A. Efficient microwave-assisted preparation of squaric acid monoamides in water. *RSC Adv.* **2013**, *3*, 7249–7253. [CrossRef]
29. Jyothish, K.; Arun, K.T.; Ramaiah, D. Synthesis of novel quinaldine-based squaraine dyes: Effect of substituents and role of electronic factors. *Org. Lett.* **2004**, *6*, 3965–3968. [CrossRef]
30. Avirah, R.R.; Jyothish, K.; Ramaiah, D. Dual-mode semisquaraine-based sensor for selective detection of Hg^{2+} in a micellar medium. *Org. Lett.* **2007**, *9*, 121–125. [CrossRef]
31. Jyothish, K.; Avirah, R.R.; Ramaiah, D. Synthesis of new cholesterol- and sugar-anchored squaraine dyes: Further evidence of how electronic factors influence dye formation. *Org. Lett.* **2006**, *8*, 111–114. [CrossRef]
32. Mahs, G.; Hegenberg, P. Synthesis and derivatives of squaric acid. *Angew. Chem. Int. Ed.* **1966**, *5*, 888–893. [CrossRef]
33. Schmidt, A.H.; Ried, W. The preparative chemistry of cylobutenediones. III. Synthesis of squaric acid, benzocyclobutenedione and their derivatives. *Synthesis* **1978**, 869–880. [CrossRef]
34. Schmidt, A.H. Reactions of squaric acid and its derivatives. *Synthesis* **1980**, 961–994. [CrossRef]
35. Röesch, A.T.; Zhu, Q.; Robben, J.; Tassinari, F.; Meskers, S.C.J.; Naaman, R.; Palmans, A.R.A.; Meijer, E.W. Helicity control in the aggregation of achiral squaraine dyes in solution and thin films. *Chem. Eur. J.* **2021**, *27*, 298–306. [CrossRef]
36. Lim, N.C.; Morton, M.D.; Jenkins, H.A.; Brückner, C. Squaric acid N-hydroxylamides: Synthesis, structure, and properties of vinylogous hydroxamic acid analogues. *J. Org. Chem.* **2003**, *68*, 9233–9241. [CrossRef] [PubMed]
37. Chan, P.C.M.; Roon, R.J.; Koerner, J.F.; Taylor, N.J.; Honek, J.F. A 3-amino-4-hydroxy-3-cyclobutene-1,2-dione-containing glutamate analog exhibiting high affinity to excitatory amino acid receptors. *J. Med. Chem.* **1995**, *38*, 4433–4438. [CrossRef] [PubMed]
38. Ivanovsky, S.A.; Dorogov, M.V.; Kravchenko, D.V.; Ivachtchenko, A.V. Synthesis of the substituted 3-cyclobutene-1,2-diones. *Synth. Commun.* **2007**, *37*, 2527–2542. [CrossRef]

39. Lunelli, B. New, optimized preparation of 1,2-dichlorocyclobuten-3,4-dione ($C_4O_2Cl_2$) from squaric acid and oxalyl chloride. *Tetrahedron Lett.* **2007**, *48*, 3595–3597. [CrossRef]
40. Garbay, G.; Tailliez, T.; Pavlopoulou, E.; Oriou, J.; Bezirdjolou, M.; Hadziioannou, G.; Cloutet, E.; Brochon, C. Triaryl-1,4-diamine-based polysquaraines: Effect of co-solvent and monomer insertion on optoelectronic properties. *Polymer Chem.* **2018**, *9*, 1288–1292. [CrossRef]
41. Schmidt, A.H.; Plaul, W.; Aimene, A.; Hotz, M.; Hoch, M. Oxocarbons and related compounds, VIII. Squaric amide chlorides: Simple methods of their preparation and cyclization of specially substituted representatives to annulated cyclobutenediones. *Liebigs Ann. Chem.* **1985**, 1021–1035. [CrossRef]
42. Chen, Z.; Zhu, Y.; Yang, D.; Zhao, S.; Zhang, L.; Yang, L.; Wu, J.; Huang, Y.; Xu, Z.; Lu, Z. An azulene-containing low bandgap small molecule for organic photovoltaics with high open circuit voltage. *Chem. Eur. J.* **2016**, *22*, 14527–14530. [CrossRef]
43. Hsueh, S.-Y.; Lai, C.-C.; Chiu, S.-H. Squaraine-based [2]rotaxanes that function as visibly active molecular switches. *Chem. Eur. J.* **2010**, *16*, 2997–3000. [CrossRef]
44. Yagi, S.; Fujie, Y.; Hyodo, Y.; Nakazumi, H. Synthesis, structure, and complexation properties with transition metal cations of a novel methane-bridged bisquarylium dye. *Dyes Pigments* **2002**, *52*, 245–252. [CrossRef]
45. Cole, E.L.; Arunkumar, E.; Xiao, S.; Smith, B.A.; Smith, B.D. Water-soluble, deep-red fluorescent squaraine rotaxanes. *Org. Biomol. Chem.* **2012**, *10*, 5769–5773. [CrossRef]
46. Schmidt, A.H.; Thiel, S.H.; Gaschler, O. Oxocarbons and related compounds. Part 24. Chlorosquarylation of indoles. *J. Chem. Soc. Perkin Trans.* **1996**, *1*, 495–496. [CrossRef]
47. Dehmlow, E.V. Preparation of 3-alkoxy-4-alkyl-3-cyclobutene-1,2-dione. *Chem. Ber.* **1980**, *113*, 1–8. [CrossRef]
48. Campbell, E.F.; Park, A.K.; Kinney, W.A.; Fengl, R.W.; Liebeskind, L.S. Synthesis of 3-hydroxy-3-cyclobutene-1,2-dione based amino acids. *J. Org. Chem.* **1995**, *60*, 1470–1472. [CrossRef]
49. Luo, C.; Zhou, Q.; Jiang, G.; He, L.; Zhang, B.; Wang, X. The synthesis of $^1O_2$ photosensitization of halogenated asymmetric aniline-based squaraines. *New. J. Chem.* **2011**, *35*, 1128–1132. [CrossRef]
50. Kaur, B.; Kaur, N.; Kumar, S. Colorimetric metal ion sensors—A comprehensive review of the years 2011–2016. *Coord. Chem. Rev.* **2018**, *358*, 13–69. [CrossRef]
51. Gokel, G.W.; Leevy, W.M.; Weber, M.E. Crown ethers: Sensors for ions and molecular scaffolds for materials and biological models. *Chem. Rev.* **2004**, *104*, 2723–2750. [CrossRef]
52. Krakowiak, K.E.; Bradshaw, J.S.; Zamecka-Krakowiak, D.J. Synthesis of aza-crown ethers. *Chem. Rev.* **1989**, *89*, 929–972. [CrossRef]
53. Das, S.; Thomas, G.; Thomas, K.J.; George, M.V.; Bedja, I.; Kamat, P.V. Crown ether derivatives of squaraine: New near-infrared-absorbing, redox-active fluorophores for alkali metal recognition. *Anal. Proc.* **1995**, *32*, 213–215. [CrossRef]
54. Lozano-Torres, B.; Marcos, M.D.; Pardo, T.; Sancenón, F.; Martínez-Máñez, R.; Rurack, K. Anilinopyridine-metal complexes for the selective chromogenic sensing of cyanide anion. *J. Coord. Chem.* **2018**, *71*, 786–796. [CrossRef]
55. Lu, X.-X.; Qin, S.-Y.; Zhou, Z.-Y.; Yam, V.W.-W. Synthesis, structure, and ion-binding studies of cobalt(II) complexes with aza-crown substituted salicylaldimine Schiff base ligand. *Inorg. Chim. Acta* **2003**, *346*, 49–56. [CrossRef]
56. Deveci, P.; Taner, B.; Ustundag, Z.; Ozcan, E.; Solak, A.O.; Kilic, Z. Synthesis, enhanced spectroscopic characterization and electrochemical grafting of N-(4-aminophenyl)aza-18-crown-6: Application of DEPT, HETCOR, HMBC-NMR and x-ray photoelectron spectroscopy. *J. Mol. Struct.* **2010**, *982*, 162–168. [CrossRef]
57. Das, S.; Thomas, K.G.; Kamat, P.V.; George, M.V. Photochemistry of squaraine dyes. 8. Photophysical properties of crown ether squaraine fluoroionophores and their metal ion complexes. *J. Phys. Chem.* **1994**, *98*, 9291–9296. [CrossRef]
58. Ros-Lis, J.V.; Martínez-Máñez, R.; Sancenón, F.; Soto, J.; Spieles, M.; Rurack, K. Squaraines as reporter units: Insights into their photophysics, protonation, and metal-ion coordination behavior. *Chem. Eur. J.* **2008**, *14*, 10101–10114. [CrossRef]
59. Ogus, U.; Akkaya, E.U. One-pot synthesis of a red-fluorescent chemosensor from an azacrown, phloroglucinol and squaric acid: A simple in-solution construction of a functional molecular device. *Tetrahedron Lett.* **1997**, *38*, 4509–4512. [CrossRef]
60. Oguz, U.; Akkaya, E.U. One-pot synthesis of squaraine fluoroionophores. *J. Org. Chem.* **1998**, *63*, 6059–6060. [CrossRef]
61. Kim, S.-H.; Han, S.-K.; Park, S.-H.; Yoon, C.-M.; Keum, S.-R. Novel fluorescent chemosensor for Li^+ based on a squarylium dye carrying a monoazacrown moiety. *Dyes Pigments* **1999**, *43*, 21–25. [CrossRef]
62. Oguz, U.; Akkaya, E.U. A squraine-based sodium selective fluorescent chemosensor. *Tetrahedron Lett.* **1998**, *39*, 5857–5860. [CrossRef]
63. Hu, L.; Zhang, Y.; Nie, L.; Xie, C.; Yan, Z. Colorimetric detection of trace Hg^{2+} with near-infrared absorbing squaraine functionalized by dibenzo-18-crown-6 and its mechanism. *Spectrochim. Acta A* **2013**, *104*, 87–91. [CrossRef] [PubMed]
64. Atilgan, S.; Kutuk, I.; Ozdemir, T. A near IR di-styryl BODIPY-based ratiometric fluorescent chemosensor for Hg(II). *Tetrahedron Lett.* **2010**, *51*, 892–894. [CrossRef]
65. Li, J.; Yim, D.; Jang, W.-D.; Yoon, J. Recent progress in the design and applications of fluorescence probes containing crown ethers. *Chem. Soc. Rev.* **2017**, *46*, 2437–2458. [CrossRef]
66. Ros-Lis, J.V.; Martínez-Máñez, R.; Rurack, K.; Sancenón, F.; Soto, J.; Spieles, M. Highly selective chromogenic signaling of Hg^{2+} in aqueous media at nanomolar levels employing a squaraine-based reporter. *Inorg. Chem.* **2004**, *43*, 5183–5185. [CrossRef] [PubMed]
67. Zhu, X.; Zheg, Q.; Wang, G.; Fu, N. Ultrasensitive detection of lead (II) based on the disaggregation of a polyether bridged squaraine fluorescent probe. *Sens. Actuators B* **2016**, *237*, 802–809. [CrossRef]
68. Manna, U.; Das, G. Positional isomeric effect of acyclic hosts on supramolecular recognition of anionic guests. *Coord. Chem. Rev.* **2021**, *440*, 213931. [CrossRef]

69. Steed, J.W. A modular approach to anion binding podands: Adaptability in properties. *Chem. Commun.* **2006**, 2637–3649. [CrossRef]
70. Jeunesse, C.; Armspach, D.; Matt, D. Playing with podands based on cone-shaped cavities. How can a cavity influence the properties of an appended metal centre? *Chem. Commun.* **2005**, 5603–5614. [CrossRef]
71. Ajayaghosh, A.; Arunkumar, E.; Daub, J. A highly specific Ca^{2+}-ion sensor: Signaling by exciton interaction in a rigid-flexible-rigid bichromophoric "H" foldamer. *Angew. Chem. Int. Ed.* **2002**, *41*, 1766–1769. [CrossRef]
72. Arunkumar, E.; Chithra, P.; Ajayaghosh, A. A controlled supramolecular approach toward cation-specific chemosensors: Alkaline earth metal ion-driven exciton signaling in squaraine tethered podands. *J. Am. Chem. Soc.* **2004**, *126*, 6590–6598. [CrossRef] [PubMed]
73. Ajayaghosh, A.; Arunkumar, E. ^{1}H NMR spectral evidence for a specific host-guest complexation induced charge localization in squaraine dyes. *Org. Lett.* **2005**, *7*, 3135–3138. [CrossRef]
74. Zhu, H.; Lin, Y.; Wang, G.; Chen, Y.; Lin, X.; Fu, N. A coordination driven deaggregation approach toward Hg^{2+}-specific chemosensors based on thioether linked squaraine-aniline dyads. *Sens. Actuators B* **2014**, *198*, 201–209. [CrossRef]
75. Chen, C.; Wang, R.; Guo, L.; Fu, N.; Dong, H.; Yan, Y. A squaraine-based colorimetric and "turn on" fluorescent sensor for selective detection of Hg^{2+} in an aqueous medium. *Org. Lett.* **2011**, *13*, 1162–1165. [CrossRef]
76. Chen, C.; Dong, H.; Chen, Y.; Guo, L.; Wang, Z.; Sun, J.-J.; Fu, N. Dual-mode unsymmetrical squaraine-based sensors for selective detection of Hg^{2+} in aqueous media. *Org. Biomol. Chem.* **2011**, *9*, 8195–8201. [CrossRef] [PubMed]
77. Fu, N.; Chen, Y.; Fan, J.; Wang, G.; Lin, S. A bifunctional "turn on" fluorescent probe for trace level Hg^{2+} and EDTA in aqueous solution via chelator promoted cation induced deaggregation signaling. *Sens. Actuators B* **2014**, *203*, 435–443. [CrossRef]
78. Zhu, H.; Fan, J.; Chen, H.; Tang, Z.; Wang, G.; Fu, N. As EDTA promoted coordination induced disaggregation for specific Hg^{2+} detection. *Dyes Pigments* **2015**, *113*, 181–188. [CrossRef]
79. Lin, S.-Y.; Zhu, H.-J.; Xu, W.-J.; Wang, G.-M.; Fu, N.-Y. A squaraine based fluorescent probe for mercury ion via coordination induced deaggregation signaling. *Chin. Chem. Lett.* **2014**, *25*, 1291–1295. [CrossRef]
80. Luo, C.; Zhou, Q.; Zhang, B.; Wang, X. A new squaraine and Hg^{2+}-based chemosensor with tunable measuring range for thiol-containing amino acids. *New J. Chem.* **2011**, *35*, 45–48. [CrossRef]
81. Luo, C.; Zhou, Q.; Lei, W.; Wang, J.; Zhang, B.; Wang, X. Supramolecular assembly of a new squaraine and β-cyclodextrin for detection of thiol-containing amino acids in water. *Supramol. Chem.* **2011**, *23*, 657–662. [CrossRef]
82. Fan, J.; Chen, C.; Lin, Q.; Fu, N. A fluorescent probe for the dual-channel detection of Hg^{2+}/Ag^{+} and its Hg^{2+}-based complex for detection of mercapto biomolecules with a tunable measuring range. *Sens. Actuators B* **2012**, *173*, 874–881. [CrossRef]
83. Tsien, R.Y. New Calcium indicators and buffers with high selectivity against magnesium and protons: Design, synthesis, and properties of prototype structures. *Biochemistry* **1980**, *19*, 2396–2404. [CrossRef]
84. Crynkiewicz, G.; Poenie, M.; Tsien, R.Y. A new general of Ca^{2+} indicators with greatly improved fluorescent properties. *J. Biol. Chem.* **1985**, *260*, 3440–3450. [CrossRef]
85. Roopa, R.; Kumar, N.; Kumar, M.; Bhalla, V. Design and applications of small molecular probes for calcium detection. *Chem. Asian J.* **2019**, *14*, 4493–4505. [CrossRef]
86. Akkaya, E.U.; Turkyilmaz, S. A squaraine-based near IR fluorescent chemosensor for calcium. *Tetrahedron Lett.* **1997**, *38*, 4513–4516. [CrossRef]
87. Elgemeie, G.H.; Azzam, R.A.; Osman, R.R. Recent advances in synthesis, metal complexes and biological evaluation of 2-aryl, 2-pyridyl and 2-pyrimidylbenzothiazoles as potential chemotherapeutics. *Inorg. Chim. Acta* **2020**, *502*, 119302. [CrossRef]
88. Karasik, A.A.; Musina, E.I.; Strelnik, I.D.; Dayanova, I.R.; Elistratova, J.G.; Mustafina, A.R.; Sinyashin, O.G. Luminescent complexes on a scaffold of P_2N_2-ligands: Design of materials for analytical and biomedical applications. *Pure Appl. Chem.* **2019**, *91*, 839–849. [CrossRef]
89. Chi, Y.; Tong, B.; Chou, P.-T. Metal complexes with pyridyl azolates: Design, preparation and applications. *Coord. Chem. Rev.* **2014**, *281*, 1–25. [CrossRef]
90. Hancock, R.D. The pyridyl group in ligand design for selective metal ion complexation and sensing. *Chem. Soc. Rev.* **2013**, *42*, 1500–1524. [CrossRef]
91. Kumar, S.; Siddhant, S.; Kumar, A.; Kumar, P. Recognition, mechanistic investigation and applications for the detection of biorelevant Cu^{2+}/Fe^{2+}/Fe^{3+} ions by ruthenium(II)-polypyridyl based fluorescent sensors. *Dalton Trans.* **2021**, *50*, 2705–2721. [CrossRef] [PubMed]
92. Kwon, N.; Hu, Y.; Yoon, J. Fluorescent chemosensors for various analytes including reactive oxygen species, biothiols, metal ions, and toxic gases. *ACS Omega* **2018**, *3*, 13731–13751. [CrossRef] [PubMed]
93. Pal, S.; Chatterjee, N.; Bharadwaj, P.K. Selective sensing first-row transition metal ions through fluorescence enhancement. *RSC Adv.* **2014**, *4*, 26585–26620. [CrossRef]
94. Esteves, C.V.; Costa, J.; Bernard, H.; Tripier, R.; Delgado, R. A squaraine-based dipicolylamine derivative acting as a turn-on mercury(II) fluorescent probe in water. *New J. Chem.* **2020**, *44*, 6589–6600. [CrossRef]
95. Storer, R.I.; Aciro, C.; Jones, L.H. Squaramides: Physical properties, synthesis and applications. *Chem. Soc. Rev.* **2011**, *40*, 2330–2346. [CrossRef] [PubMed]
96. Wang, W.; Fu, A.; You, J.; Gao, G.; Lan, J.; Chen, L. Squaraine-based colorimetric and fluorescent sensors for Cu^{2+}-specific detection and fluorescence imaging in living cells. *Tetrahedron* **2010**, *66*, 3695–3701. [CrossRef]

97. Lin, Q.; Huang, Y.; Fan, J.; Wang, R.; Fu, N. A squaraine and Hg^{2+}-based colorimetric and "turn on" fluorescent probe for cysteine. *Talanta* **2013**, *114*, 66–72. [CrossRef] [PubMed]
98. Huang, T.; Lin, Q.; Wu, J.; Fu, N. Design and synthesis of a squaraine based near-infrared fluorescent probe for the ratiometric detection of Zn^{2+} ions. *Dyes Pigments* **2013**, *99*, 699–704. [CrossRef]
99. Xia, G.; Liu, Y.; Ye, B.; Sun, J.; Wang, H. A squaraine-based colorimetric and F^- dependent chemosensor for recyclable CO_2 gas detection: Highly sensitive off-on-off response. *Chem. Commun.* **2015**, *51*, 13802–13805. [CrossRef] [PubMed]
100. Sun, J.; Ye, B.; Xia, G.; Zhao, X.; Wang, H. A colorimetric and fluorescent chemosensor for the highly sensitive detection of CO_2 gas: Experiment and DFT calculation. *Sens. Actuators B* **2016**, *233*, 76–82. [CrossRef]
101. Wang, F.; Wang, L.; Chen, X.; Yoon, J. Recent progress in the development of fluorometric and colorimetric chemosensors for detection of cyanide ions. *Chem. Soc. Rev.* **2014**, *43*, 4312–4324. [CrossRef] [PubMed]
102. Mondal, A.; Nag, S.; Banerjee, P. Coumarin functionalized molecular scaffolds for the effectual detection of hazardous fluoride and cyanide. *Dalton Trans.* **2021**, *50*, 429–451. [CrossRef] [PubMed]
103. Hewage, H.S.; Anslyn, E.V. Pattern-based recognition of thiols and metals using a single squaraine indicator. *J. Am. Chem. Soc.* **2009**, *131*, 13099–13106. [CrossRef]
104. Sklavounos, A.A.; Pefkianakis, E.K.; Toubanaki, D.T.; Vougiokalakis, G.C.; Calokerinos, A.C. A squaraine derivative for cost-effective, quick, and highly sensitive determination of mercury and thiols and pH sensing. *ChemPusChem* **2016**, *81*, 913–916. [CrossRef] [PubMed]
105. Ros-Lis, J.V.; Garcia, B.; Jimenez, D.; Martínez-Máñez, R.; Sancenón, F.; Soto, J.; Gonzalvo, F.; Valldecabres, M.C. Squaraines as fluoro-chromogenic probes for thiol-containing compounds and their application to the detection of biorelevant thiols. *J. Am. Chem. Soc.* **2004**, *126*, 4064–4065. [CrossRef]
106. Chua, M.H.; Zhou, H.; Lin, T.T.; Wu, J.; Xu, J. Triphenylethylene- and tetraphenylethylene-functionalized 1,3-bis(pyrrol-2-yl)squaraine dyes: Synthesis, aggregation-caused quenching to aggregation-induced emission, and thiol detection. *ACS Omega* **2018**, *3*, 16424–16435. [CrossRef]
107. Liu, T.; Yang, L.; Zhang, J.; Liu, K.; Ding, L.; Peng, H.; Belfield, K.D.; Fang, Y. Squaraine-hydrazine adducts for fast and colorimetric detection of aldehydes in aqueous media. *Sens. Actuators B* **2019**, *292*, 88–93. [CrossRef]
108. Ros-Lis, J.V.; Martínez-Máñez, R.; Soto, J. A selective chromogenic reagent for cyanide determination. *Chem. Commun.* **2002**, 2248–22249. [CrossRef]
109. Liu, T.; Liu, X.; Valencia, M.A.; Sui, B.; Zhang, Y.; Belfield, K.D. Far-red-emitting TEG-substituted squaraine dye: Synthesis, optical properties, and selective detection of cyanide in aqueous solution. *Eur. J. Org. Chem.* **2017**, *2017*, 3957–3964. [CrossRef]
110. Wright, A.T.; Anslyn, E.V. Differential receptor arrays and assays for solution-based molecular recognition. *Chem. Soc. Rev.* **2006**, *35*, 14–28. [CrossRef]
111. Severin, K. Pattern-based sensing with simple metal-dye complexes. *Curr. Opin. Chem. Biol.* **2010**, *14*, 737–742. [CrossRef]
112. Yu, H.; Fu, M.; Xiao, Y. Switching off FRET by analyte-induced decomposition of squaraine energy acceptor: A concept to transform 'turn off' chemodosimeter into ratiometirc sensors. *Phys. Chem. Chem. Phys.* **2010**, *12*, 7386–7391. [CrossRef]
113. Bacher, E.P.; Lepore, A.J.; Pena-Romero, D.; Smith, D.B.; Ashfeld, B. Nucleophilic addition of phosphorus (III) derivatives to squaraines: Colorimetric detection of transition metal-mediated or thermal reversion. *Chem. Commun.* **2019**, *55*, 3286–3289. [CrossRef] [PubMed]
114. Bacher, E.P.; Koh, K.J.; Lepore, A.J.; Oliver, A.G.; Wiest, O.; Ashfeld, B.L. A phosphine-mediated dearomative skeletal rearrangement of dianiline squaraine dyes. *Org. Lett.* **2021**, *23*, 2853–2857. [CrossRef] [PubMed]
115. Gassensmith, J.J.; Baumes, J.M.; Smith, B.D. Discovery and early development of squaraine rotaxane. *Chem. Commun.* **2009**, 6329–6338. [CrossRef] [PubMed]
116. Schreiber, C.L.; Zhai, C.; Dempsey, J.M.; McGarraugh, H.H.; Matthews, B.P.; Christmann, C.R.; Smith, B.D. Paired agent fluorescence imaging of cancer in a living mouse using preassembled squaraine molecular probes with emission wavelengths of 690 and 830 nm. *Bioconjugate Chem.* **2020**, *31*, 214–223. [CrossRef]
117. Shaw, S.K.; Liu, W.; Gomez Duran, C.F.A.; Schreiber, C.L.; de Lourdes Batacount Mendiola, M.; Zhai, C.; Roland, F.M.; Padanilam, S.J.; Smith, B.D. Non-covalently pre-assembled high-performance near-infrared fluorescent molecular probes. *Chem. Eur. J.* **2018**, *24*, 13821–13829. [CrossRef]
118. Lee, J.-J.; White, A.G.; Rice, D.R.; Smith, B.D. In vivo imaging using polymeric nanoparticles stained with near-infrared chemiluminescent and fluorescent squaraine catenane endoperoxide. *Chem. Commun.* **2013**, *49*, 3016–3018. [CrossRef]
119. Diehl, K.; Bachman, J.L.; Anslyn, E.V. Tuning thiol addition to squaraines by *ortho*-substitution and the use of serum albumin. *Dyes Pigments* **2017**, *141*, 316–324. [CrossRef]
120. Karpenko, I.A.; Klymchenko, A.S.; Gioria, S.; Kreder, R.; Shulov, L.; Villa, P.; Mély, Y.; Hibert, M.; Bonnet, D. Squaraine as a bright, stable and environment-sensitive far-red label for receptor-specific cellular imaging. *Chem. Commun.* **2015**, *51*, 2960–2963. [CrossRef] [PubMed]
121. Liu, Y.; Yu, Y.; Zhao, Q.; Tang, C.; Zhang, H.; Qin, Y.; Feng, X.; Zhang, J. Fluorescent probes based on nucleophilic aromatic substitution reactions for reactive sulfur and selenium species: Recent progress, applications, and design strategies. *Coord. Chem. Rev.* **2021**, *427*, 213601. [CrossRef]
122. Peng, H.; Chen, W.; Cheng, Y.; Hakuna, L.; Strongin, R.; Wang, B. Thiol reactive probes and chemosensors. *Sensors* **2012**, *12*, 15907–15946. [CrossRef]

123. Shibata, A.; Abe, H.; Ito, M.; Kondo, Y.; Shimizu, S.; Aikawa, K.; Ito, Y. DNA template nucleophilic aromatic substitution reactions for fluorogenic sensing of oligonucleotides. *Chem. Commun.* **2009**, 6586–6588. [CrossRef] [PubMed]
124. Zhang, J.; Shibata, A.; Ito, M.; Shuto, S.; Ito, Y.; Mannervik, B.; Abe, H.; Morgenstern, R. Synthesis and characterization of a series of highly fluorogenic substrates for glutathione transferases, a general strategy. *J. Am. Chem. Soc.* **2011**, *133*, 14109–14119. [CrossRef] [PubMed]
125. Liu, X.-D.; Sun, R.; Ge, J.-F.; Xu, Y.-J.; Xu, Y.; Lu, J.-M. A squaraine-based red emission off-on chemosensor for biothiols and its application in living cells imaging. *Org. Biomol. Chem.* **2013**, *11*, 4258–4264. [CrossRef]
126. Xiong, L.; Ma, J.; Huang, Y.; Wang, Z.; Lu, Z. Highly sensitive squaraine-based water-soluble far-red/near-infrared chromofluorogenic thiophenol probe. *ACS Sens.* **2017**, *2*, 599–605. [CrossRef] [PubMed]
127. Jiang, W.; Fu, Q.; Fan, H.; Ho, J.; Wang, W. A highly selective fluorescent probe for thiophenols. *Angew. Chem. Int. Ed.* **2007**, *46*, 8445–8448. [CrossRef]
128. Jiang, W.; Cao, Y.; Liu, Y.; Wang, W. Rational design of a highly selective and sensitive fluorescent PET probe for discrimination of thiophenols and aliphatic thiols. *Chem. Commun.* **2010**, *46*, 1944–1946. [CrossRef]
129. Wang, G.; Xu, W.; Yang, H.; Fu, N. Highly sensitive and selective strategy for imaging Hg^{2+} using near-infrared squaraine dye in live cells and zebrafish. *Dyes Pigments* **2018**, *157*, 369–376. [CrossRef]
130. Ozturk, T.; Ertas, E.; Mert, O. Use of Lawesson's reaction in organic synthesis. *Chem. Rev.* **2007**, *107*, 5210–5278. [CrossRef] [PubMed]
131. Philips, D.S.; Ghosh, S.; Sudheesh, K.V.; Suresh, C.H.; Ajayaghosh, A. An unsymmetrical squaraine-dye-based chemical platform for multiple analyte recognition. *Chem. Eur. J.* **2017**, *23*, 17973–17980. [CrossRef] [PubMed]